



ISIMIP3b bias adjustment fact sheet

Stefan Lange
February 27, 2020

Contents

1	Introduction	1
2	Observational dataset	1
3	Bias adjustment and statistical downscaling method	1
4	Preprocessing of climate model output	4
5	Climate model selection	4
6	Results	6

If you use bias-adjusted ISIMIP3b climate input data then please cite (where applicable) Lange (2019a) and Lange (2020) for the bias adjustment and statistical downscaling method ISIMIP3BASD, and Lange (2019b) and Cucchi et al. (2020) and for the observational dataset W5E5.

Table 1: Specs of climate variables bias-adjusted and statistically downscaled for ISIMIP3b. Note that the upper limits of pr and prsn correspond to 600 mm day^{-1} and 300 mm day^{-1} , respectively, while the lower and upper limits of tas, tasmax and tasmin correspond to -90°C and $+70^\circ\text{C}$, respectively.

Variable	Short name	Unit	Limits
Near-Surface Relative Humidity	hurs	%	[1, 100]
Near-Surface Specific Humidity	huss	kg kg^{-1}	[0.0000001, 0.1]
Precipitation	pr	$\text{kg m}^{-2} \text{s}^{-1}$	[0, 0.0069444444]
Snowfall Flux	prsn	$\text{kg m}^{-1} \text{s}^{-1}$	[0, 0.0034722222]
Surface Air Pressure	ps	Pa	[480, 110000]
Surface Downwelling Longwave Radiation	rlds	W m^{-2}	[40, 600]
Surface Downwelling Shortwave Radiation	rsds	W m^{-2}	[0, 500]
Near-Surface Wind Speed	sfcWind	m s^{-1}	[0.1, 50]
Near-Surface Air Temperature	tas	K	[183.15, 343.15]
Daily Maximum Near-Surface Air Temperature	tasmax	K	[183.15, 343.15]
Daily Minimum Near-Surface Air Temperature	tasmin	K	[183.15, 343.15]

1 Introduction

This document describes the climate model selection, bias adjustment and statistical downscaling that was carried out to produce the climate input data for phase 3b of the Inter-Sectoral Impact Model Intercomparison Project (ISIMIP3b) based on output of phase 6 of the Coupled Model Intercomparison Project (CMIP6; Eyring et al., 2016). The document is structured as follows. It first describes the observational dataset (Sect. 2) and the methods (Sect. 3) used for bias adjustment and statistical downscaling. It then outlines how climate model output was preprocessed (Sect. 4) and how climate models were grouped into primary and secondary models (Sect. 5) and concludes with the discussion of selected results (Sect. 6).

2 Observational dataset

The observational reference dataset used for bias adjustment and statistical downscaling in ISIMIP3b is version 1.0 of WFDE5 over land merged with ERA5 over the ocean (W5E5; Lange, 2019b; Cucchi et al., 2020). This dataset covers 1979–2016 at daily temporal resolution and the entire globe at 0.5° spatial resolution. Data sources of W5E5 are version 1.0 of WATCH Forcing Data methodology applied to ERA5 data (WFDE5; Weedon et al., 2014; Cucchi et al., 2020), ERA5 reanalysis data (Hersbach et al., 2019), and precipitation data from version 2.3 of the Global Precipitation Climatology Project (GPCP; Adler et al., 2003).

3 Bias adjustment and statistical downscaling method

The method used for bias adjustment and statistical downscaling in ISIMIP3b is version 2.3 of ISIMIP3BASD (Lange, 2019a, 2020). Table 1 lists all variables that were adjusted and downscaled. From these variables, huss, prsn, tasmax and tasmin were adjusted and downscaled indirectly: huss was derived from adjusted and downscaled hurs, ps and tas, prsn was derived from adjusted and downscaled pr and prsnratio = prsn/pr, and tasmax and tasmin were derived from adjusted and downscaled tas, tasrange = tasmax – tasmin and tasskew = (tas – tasmin)/(tasmax – tasmin).

Compared to version 1.0 of ISIMIP3BASD described in Lange (2019a), version 2.3 features (i) multiple minor bug fixes, (ii) detrending conditional on linear trends being significantly different from 0 at the 5 % level, (iii) trend-aware replacement of missing values, which is relevant for prsnratio as this variable has missing values whenever pr = 0, (iv) improved randomization of values beyond threshold for a better bias adjustment of hurs in cases of many values beyond 100 %, (v) non-parametric quantile mapping for a more robust bias adjustment of bounded variables, (vi) revised formulas (8) and (9)

Table 2: Specs of CMIP6 climate models included in ISIMIP3b. Primary models are mandatory to use by the ISIMIP impact modelling teams. Secondary models are optional. The third column shows the spatial resolution that the original data was interpolated to prior to bias adjustment and statistical downscaling. The fourth column shows which ensemble member was used. The fifth column shows which year labels were attached to the original piControl data used for ISIMIP3b. The last two columns indicate whether ps and sfcWind data were directly available or needed to be approximated from other available output using Eq. (1) for ps and Eq. (2) for sfcWind. Note that the model order in this table is alphabetical, i.e., no ranking within the groups is implied.

Model	Group	Resolution	Member	piControl	ps	sfcWind
GFDL-ESM4	primary	1.0°	r1i1p1f1	0001–0500	available	available
IPSL-CM6A-LR	primary	2.0°	r1i1p1f1	1870–2369	available	available
MPI-ESM1-2-HR	primary	1.0°	r1i1p1f1	1850–2349	available	available
MRI-ESM2-0	primary	1.0°	r1i1p1f1	1850–2349	proxy	available
UKESM1-0-LL	primary	2.0°	r1i1p1f2	1960–2459	available	available
CanESM5	secondary	2.0°	r1i1p1f1	5201–5700	proxy	available
CNRM-CM6-1	secondary	1.0°	r1i1p1f2	1850–2349	proxy	proxy
CNRM-ESM2-1	secondary	1.0°	r1i1p1f2	1850–2140	proxy	proxy
EC-Earth3	secondary	0.5°	r1i1p1f1	2259–2758	proxy	available
MIROC6	secondary	1.0°	r1i1p1f1	3200–3699	proxy	proxy

of Lange (2019a) for a better bias adjustment of bounded variables and frequencies of values beyond threshold, and (vii) multivariate bias adjustment based on the MBCn algorithm by Cannon (2017).

Feature (vii) was not used in ISIMIP3b though because it produced overfitting artifacts that were deemed too serious to tolerate. Univariate bias adjustment was used instead. Also to avoid overfitting artifacts, event likelihood adjustments as described in Lange (2019a) were not applied. Lastly, to avoid unstable beta distribution fits, bounded variables (hurs, prsnratio, rsds, tasskew) were bias adjusted using non-parametric quantile mapping.

The training period used for both bias adjustment and statistical downscaling was 1979–2014. Like the training period, all application periods have a length of 36 years. Application periods used for piControl were 1601–1636, 1637–1672, 1673–1708, 1709–1744, 1745–1780, 1781–1816, 1817–1852, 1853–1888, 1889–1924, 1925–1960, 1961–1996, 1997–2032, 2033–2068 (keeping 2033–2066), and 2065–2100 (keeping 2067–2100). Application periods used for historical were 1850–1885, 1886–1921, 1922–1957, 1958–1993, and 1994–2029 (combining historical and ssp585, keeping 1994–2014). Application periods used for ssp585 and ssp126 were 2015–2050 (keeping 2015–2043), 2040–2075 (keeping 2044–2072), and 2065–2100 (keeping 2073–2100). The training period was not used as an application period to avoid overfitting artifacts.

Before bias adjustment and statistical downscaling, original CMIP6 output was interpolated in time and space. In order to harmonize calendars to the proleptic Gregorian calendar, missing days were inserted using linear interpolation in time. The spatial interpolation was necessary to make the ISIMIP3BASD statistical downscaling method applicable. It was done using first-order conservative remapping (Jones, 1999) to a regular latitude–longitude grid with 0.5°, 1.0° or 2.0° resolution, depending on which was closest to the resolution of the original output (Table 2 shows which resolution was used for which climate model).

Data interpolated to 0.5° were bias-adjusted using W5E5 data at 0.5° spatial resolution. Data interpolated to 1.0° were first bias-adjusted using W5E5 data aggregated to 1.0° and then downscaled to 0.5° using W5E5 data at 0.5° spatial resolution. Data interpolated to 2.0° were first bias-adjusted using W5E5 data aggregated to 2.0° and then downscaled in two steps using W5E5 data at 1.0° and 0.5° spatial resolution. See Figure 1 and Figure 2 for python commands used for bias adjustment and statistical downscaling, respectively.

After bias adjustment and statistical downscaling, the limits listed in Table 1 were enforced for all variables, i.e., values greater/less than the upper/lower limit were set to the upper/lower limit.

```

python bias_adjustment.py
--randomization-seed 0
-v relative_humidity,precipitation_flux,snowfall_flux,surface_air_pressure,
surface_downwelling_longwave_flux_in_air,surface_downwelling_shortwave_flux_in_air,
wind_speed,air_temperature,air_temperature,air_temperature
--lower-bound 0,0,0,,,0,0,,0,0
--lower-threshold .01,.0000011574,.0001,,,0001,.01,,.01,.0001
--upper-bound 100,,1,,,1,,,1
--upper-threshold 99.99,,.9999,,.9999,,.9999
--distribution ,gamma,,normal,normal,,weibull,normal,rice,
-t bounded,mixed,bounded,additive,additive,bounded,mixed,additive,mixed,bounded
-d ,,,1,1,,,1,,
-w 0,0,0,0,0,15,0,0,0,0
--if-all-invalid-use ,,0.,,,,,,
-o OBSinput/hurs_lowres_1979-2014.nc,OBSinput/pr_lowres_1979-2014.nc,
OBSinput/prsnratio_lowres_1979-2014.nc,OBSinput/ps_lowres_1979-2014.nc,
OBSinput/rlds_lowres_1979-2014.nc,OBSinput/rsds_lowres_1979-2014.nc,
OBSinput/sfcWind_lowres_1979-2014.nc,OBSinput/tas_lowres_1979-2014.nc,
OBSinput/tasrange_lowres_1979-2014.nc,OBSinput/tasskew_lowres_1979-2014.nc
-s GCMinput/hurs_lowres_1979-2014.nc,GCMinput/pr_lowres_1979-2014.nc,
GCMinput/prsnratio_lowres_1979-2014.nc,GCMinput/ps_lowres_1979-2014.nc,
GCMinput/rlds_lowres_1979-2014.nc,GCMinput/rsds_lowres_1979-2014.nc,
GCMinput/sfcWind_lowres_1979-2014.nc,GCMinput/tas_lowres_1979-2014.nc,
GCMinput/tasrange_lowres_1979-2014.nc,GCMinput/tasskew_lowres_1979-2014.nc
-f GCMinput/hurs_lowres_2065-2100.nc,GCMinput/pr_lowres_2065-2100.nc,
GCMinput/prsnratio_lowres_2065-2100.nc,GCMinput/ps_lowres_2065-2100.nc,
GCMinput/rlds_lowres_2065-2100.nc,GCMinput/rsds_lowres_2065-2100.nc,
GCMinput/sfcWind_lowres_2065-2100.nc,GCMinput/tas_lowres_2065-2100.nc,
GCMinput/tasrange_lowres_2065-2100.nc,GCMinput/tasskew_lowres_2065-2100.nc
-b GCMoutput/hurs_lowres_2065-2100.nc,GCMoutput/pr_lowres_2065-2100.nc,
GCMoutput/prsnratio_lowres_2065-2100.nc,GCMoutput/ps_lowres_2065-2100.nc,
GCMoutput/rlds_lowres_2065-2100.nc,GCMoutput/rsds_lowres_2065-2100.nc,
GCMoutput/sfcWind_lowres_2065-2100.nc,GCMoutput/tas_lowres_2065-2100.nc,
GCMoutput/tasrange_lowres_2065-2100.nc,GCMoutput/tasskew_lowres_2065-2100.nc

```

Figure 1: Python command used for bias adjustment of all variables listed in Table 1. Note that this is stylized for the application period 2065–2100.

```

python statistical_downscaling.py
--randomization-seed 0
-v relative_humidity
--lower-bound 0
--lower-threshold .01
--upper-bound 100
--upper-threshold 99.99
-o OBSinput/hurs_highres_1979-2014.nc
-s GCMoutput/hurs_lowres_2065-2100.nc
-f GCMoutput/hurs_highres_2065-2100.nc

```

Figure 2: Python command used for statistical downscaling of hurs. Note that this is stylized for the application period 2065–2100.

4 Preprocessing of climate model output

Next to the temporal and spatial interpolation already mentioned in Sect. 3, raw CMIP6 output was harmonized in terms of variable coverage and piControl periods.

If for a given model ps data were not available for at least one experiment but psl (Sea Level Pressure) data were available for all experiments then a proxy of ps was used for all experiments. This proxy was computed according to

$$ps = psl \exp^{-1} \left(\frac{g \text{ orog}}{R \text{ tas}} \right), \quad (1)$$

where orog is the climate model orography, g is gravity and R is the specific gas constant of dry air. Similarly, if sfcWind data were not available for at least one experiment but uas and vas (Eastward and Northward Near-Surface Wind) data were available for all experiments then a proxy of sfcWind was used for all experiments. This proxy was computed according to

$$\text{sfcWind} = \sqrt{\text{uas}^2 + \text{vas}^2}. \quad (2)$$

Whether ps and sfcWind data were directly available or needed to be approximated for a given model is shown in Table 2.

Since piControl starts in different years for different models, piControl data were shifted in time to a harmonized ISIMIP3b piControl period of 1601–2100. The original piControl periods used are shown in Table 2. If fewer than 500 years worth of piControl data were available for a given model then the available data were recycled until 500 years were reached. This was only necessary for CNRM-ESM2-1, which provided 291 years worth of piControl data.

5 Climate model selection

CMIP6 experiments used in ISIMIP3b are piControl, historical, ssp126 and ssp585. In order to be included in ISIMIP3b, a climate model had to provide daily data for all variables listed in Table 1 except huss (not needed), ps (if psl was available) and sfcWind (if uas and vas were available) for at least 250 years in piControl and for all years in historical (1850–2014), ssp126 and ssp585 (2015–2100).

The models fulfilling these data availability criteria were divided into primary and secondary models. The list of primary models was fixed at the beginning of ISIMIP3b. These models are mandatory to use by the ISIMIP impact modelling teams. The list of secondary models is open and can be extended as more CMIP6 output becomes available during ISIMIP3b. These models are optional to use. The selection of primary models was done taking into account process representation, structural independence, climate sensitivity, performance in the historical period as well as the special input data needs of the fisheries and marine ecosystems sector (FishMIP).

Performance in the historical period was assessed using the portrait plot depicted in Figure 3. According to this plot, the better-performing CMIP6 models are *AWI-CM-1-1-MR*, *CESM2*, *CESM2-WACCM*, *GFDL-CM4*, GFDL-ESM4, *HadGEM3-GC31-LL*, MPI-ESM1-2-HR, *MPI-ESM1-2-LR*, MRI-ESM2-0, *SAM0-UNICON* and UKESM1-0-LL. In the previous list, models in italics are those which did not provide all data needed in ISIMIP3b. This leaves GFDL-ESM4, MPI-ESM1-2-HR, MRI-ESM2-0 and UKESM1-0-LL as potential primary models. Three of these also provide data for the essential ocean variables for FishMIP. Another model providing data for these variables is IPSL-CM6A-LR. It was decided that these five models are the primary models of ISIMIP3b.

The five primary models are a good choice because they are structurally independent in terms of their ocean and atmosphere model components and because, according to an informal survey among experts from the CRESCENDO project, their process representation is fair (IPSL-CM6A-LR, MPI-ESM1-2-HR) to good (GFDL-ESM4, MRI-ESM2-0, UKESM1-0-LL). In terms of climate sensitivity (Figure 4), the five primary models are good representatives of the whole CMIP6 ensemble as they include three models with low climate sensitivity (GFDL-ESM4, MPI-ESM1-2-HR, MRI-ESM2-0) and two models with high climate sensitivity (IPSL-CM6A-LR, UKESM1-0-LL). Also, three models (GFDL-ESM4, IPSL-CM6A-LR, UKESM1-0-LL) are successors of models used in ISIMIP2b and in the ISIMIP Fast Track, which is beneficial in terms of tracibility.

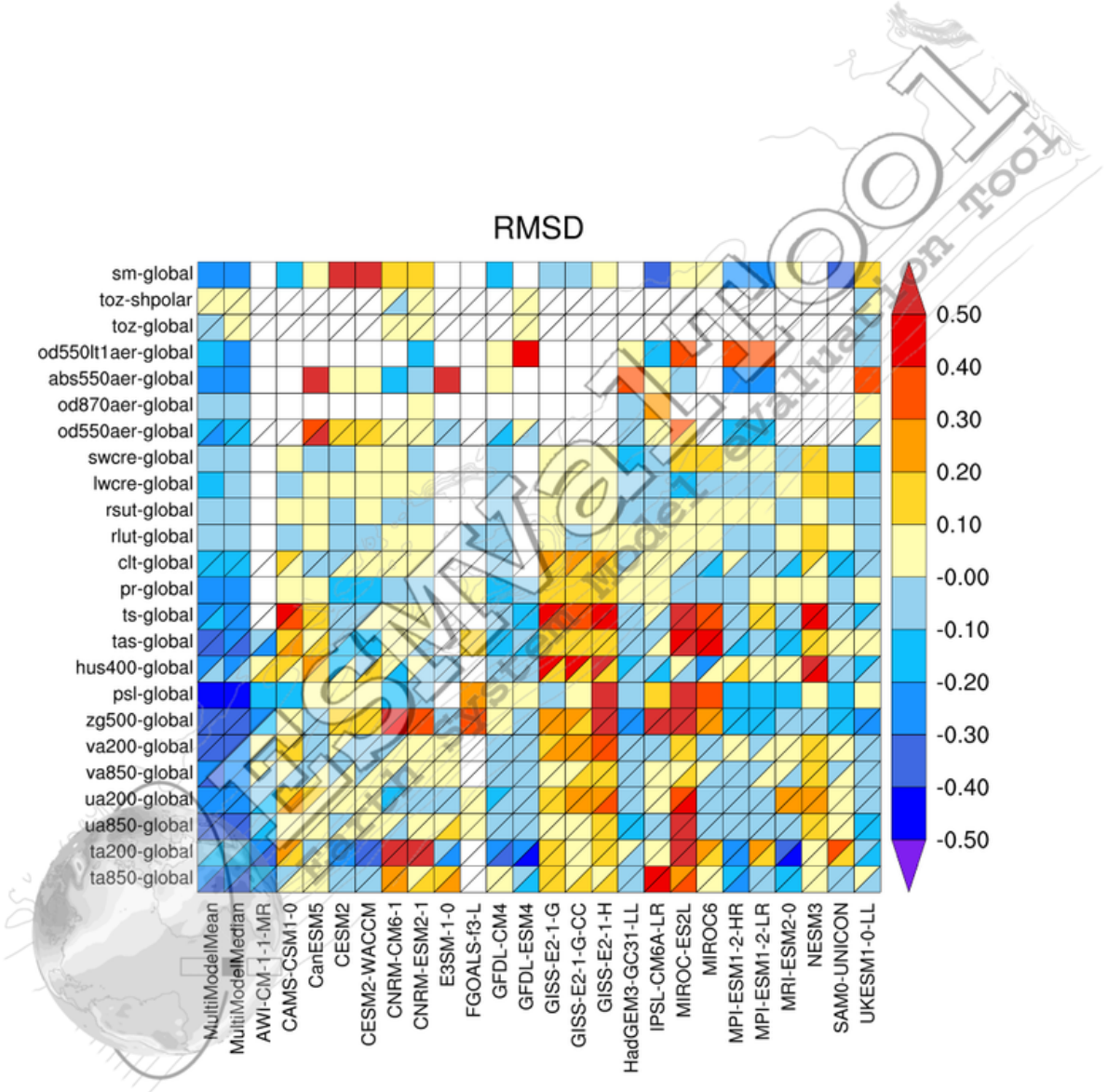


Figure 3: Portrait plot (Gleckler et al., 2008) of CMIP6 climate model performance for different models (columns) and variables (rows). The metric used as the basis of the plot is the root mean square difference (RMSD) between historical simulation and observation. Where cells are divided into triangles, two observational reference datasets were used. Monthly mean climatologies were used to compute the RMSD. These were then aggregated over calendar months and grid cells. Aggregation over all grid cells are indicated by the suffix -global, those over southern hemisphere polar grid cells only ($60\text{--}90^\circ\text{S}$) by -shpolar. RMSDs are expressed relative to the median model RMSD. White triangles or squares are due to missing data. Variables included are (from top to bottom) sm (Soil Moisture), toz (Total Ozone Column), od550lt1aer (Ambient Fine Aerosol Optical Depth at 550 nm), abs550aer (Ambient Aerosol Absorption Optical Thickness at 550 nm), od870aer (Ambient Aerosol Optical Depth at 870 nm), od550aer (Ambient Aerosol Optical Thickness at 550 nm), swcre (Shortwave Cloud Radiative Effect), lwcre (Longwave Cloud Radiative Effect), rsut (Top-of-Atmosphere Outgoing Shortwave Radiation), rlut (Top-of-Atmosphere Outgoing Longwave Radiation), clt (Total Cloud Cover Percentage), pr (Precipitation), tas (Near-Surface Air Temperature), hus400 (Specific Humidity at 400 hPa), psl (Sea Level Pressure), zg500 (Geopotential Height at 500 hPa), va200 (Northward Wind at 200 hPa), va850 (Northward Wind at 850 hPa), ua200 (Eastward Wind at 200 hPa), ua850 (Eastward Wind at 850 hPa), ta200 (Air Temperature at 200 hPa), ta850 (Air Temperature at 850 hPa). This plot was created on January 24, 2020 with ESMValTool v2.0.0b2.

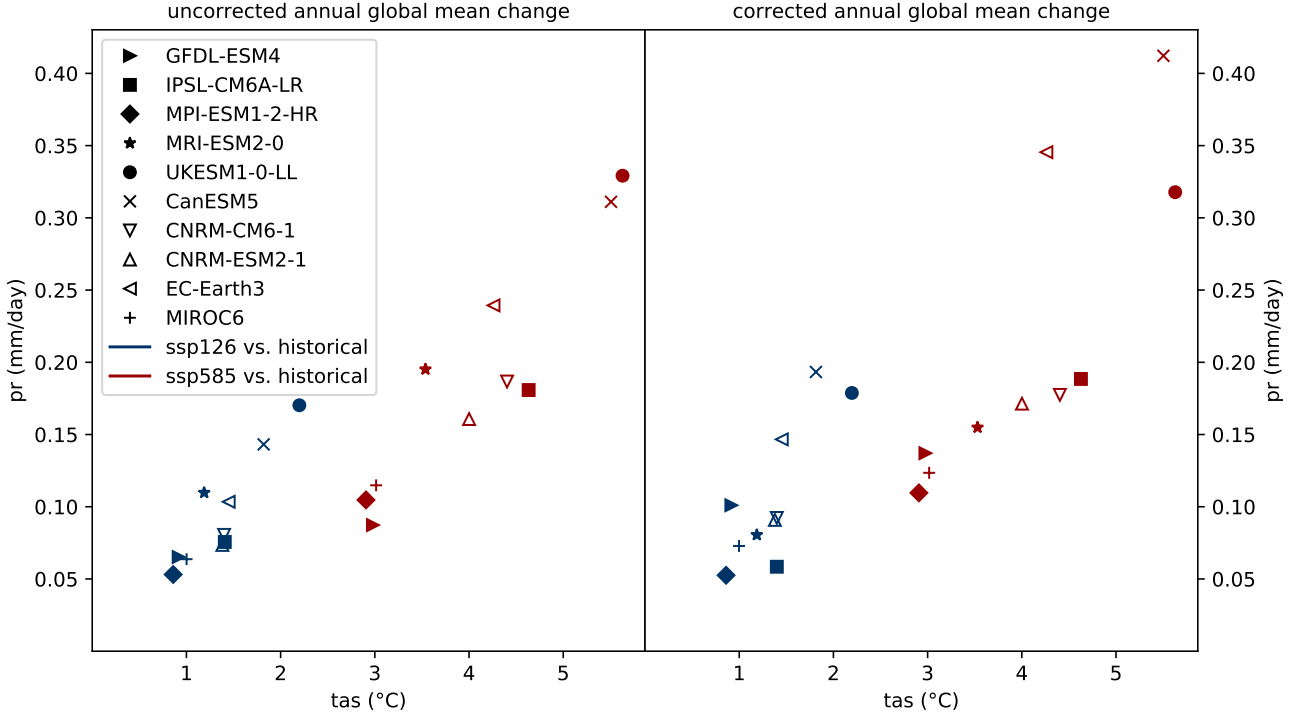


Figure 4: Projected change in annual global mean precipitation versus temperature computed based on uncorrected (left) and corrected (right) CMIP6 data. Results for different climate models are indicated with different symbols. For the primary models, these symbols are filled. Results for different future greenhouse gas emissions scenarios are indicated with different colors. Changes are computed as the difference between 30-year mean values (2071–2100 versus 1985–2014).

6 Results

Bias adjustment and statistical downscaling results are shown here using only a few selected control plots. Figure 4 shows projected changes in annual global mean precipitation and temperature before and after bias adjustment and statistical downscaling. The results demonstrate the ISIMIP3BASD preserves the simulated warming signal. Since ISIMIP3BASD preserves precipitation trends multiplicatively in most cases, the bias adjustment has altered absolute precipitation changes. The plot also shows that the spectrum of simulated global mean temperature changes is well represented by the primary models.

Time series of global annual mean values before and after bias adjustment and statistical downscaling are shown in Figures 5, 8, 11, 14, 17, 20, 23, 26, 29 and 32 for all variables listed in Table 1 and all models listed in Table 2. They demonstrate that mean values were well adjusted in most cases. Biases only remain for prsn. In addition, for CanESM5, there are discontinuities visible in the prsn time series under ssp585.

Similar plots for global annual minimum values are shown in Figures 6, 9, 12, 15, 18, 21, 24, 27, 30 and 33. The adjustment of minimum values worked well for ps, pr, prsn, rsds, tas, tasmax and tasmin. It did not work too well for hurs, huss, sfcWind and rlds as for these variables rather often the limits given in Table 1 had to be enforced in post-processing. Reasons for this include the general imperfection of parametric quantile mapping, the imperfect generation of pseudo future observations (Lange, 2019a) and the alteration of bias-adjusted values by statistical downscaling.

Time series of global annual maximum values are shown in Figures 7, 10, 13, 16, 19, 22, 25, 28, 31 and 34. The adjustment of maximum values worked well for huss, ps, rsds, tas and tasmin. It worked rather well for rlds. It did not work too well for hurs, pr, prsn, sfcWind and tasmax as for these variables rather often the limits given in Table 1 had to be enforced in post-processing, for the same reasons as in the case of the global annual minimum values.

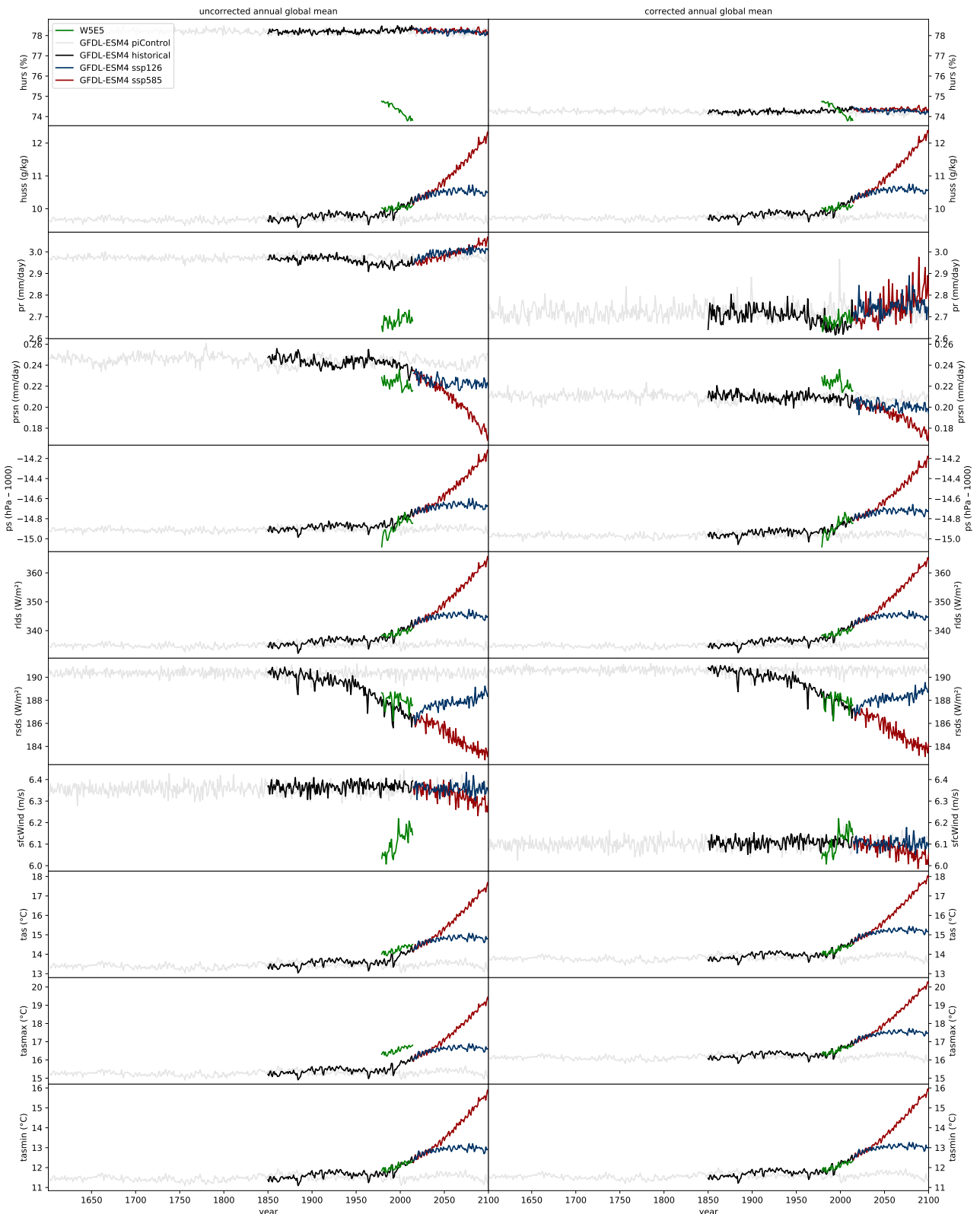


Figure 5: Uncorrected (left) and corrected (right) time series of annual global mean hurs, huss, pr, prsn, ps, rlds, rsds, sfcWind, tas, tasmax and tasmin (from top to bottom) for W5E5 (green) and GFDL-ESM4 (other colors for different CMIP6 experiments).

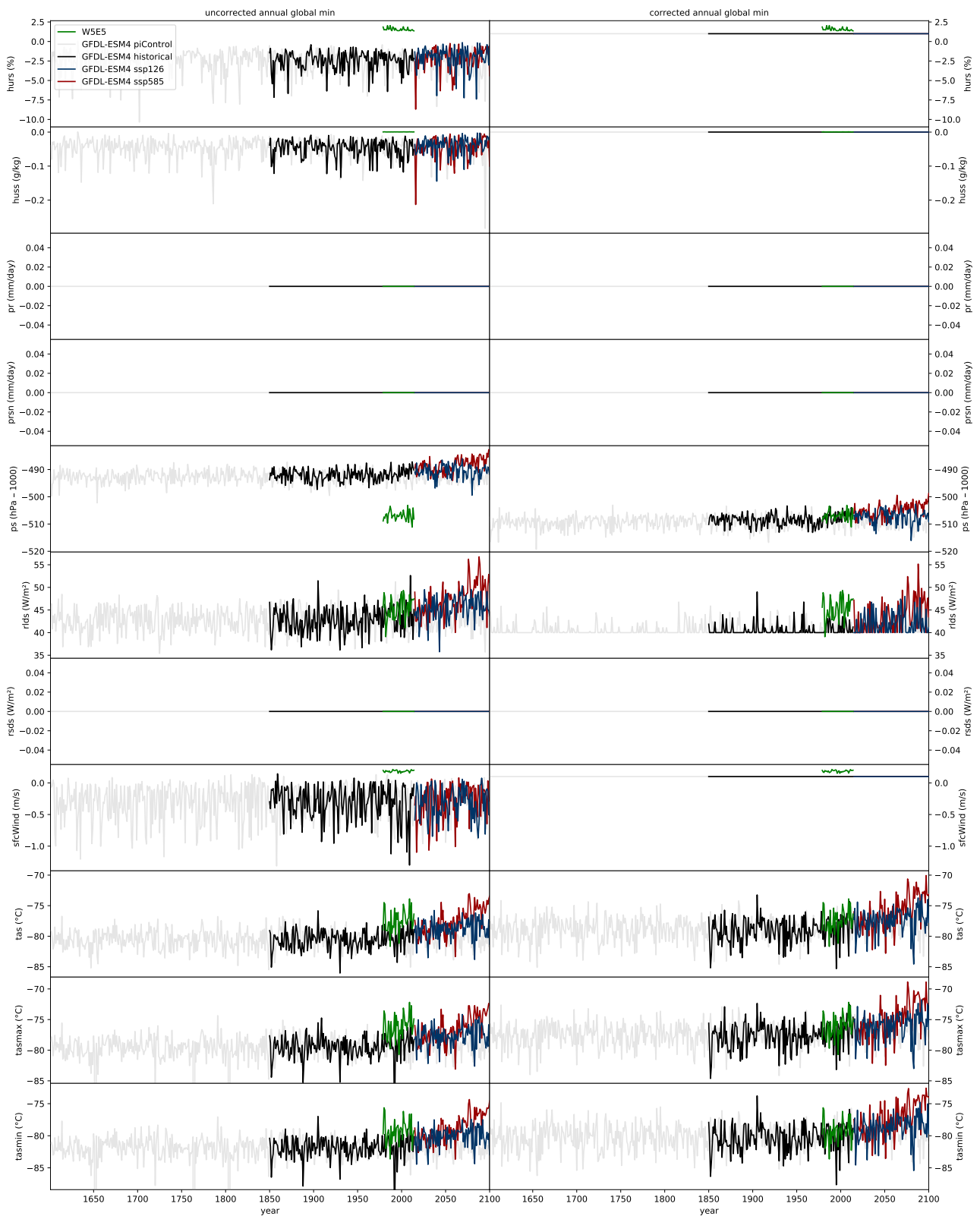


Figure 6: Same as Figure 5 but for annual global minimum values.

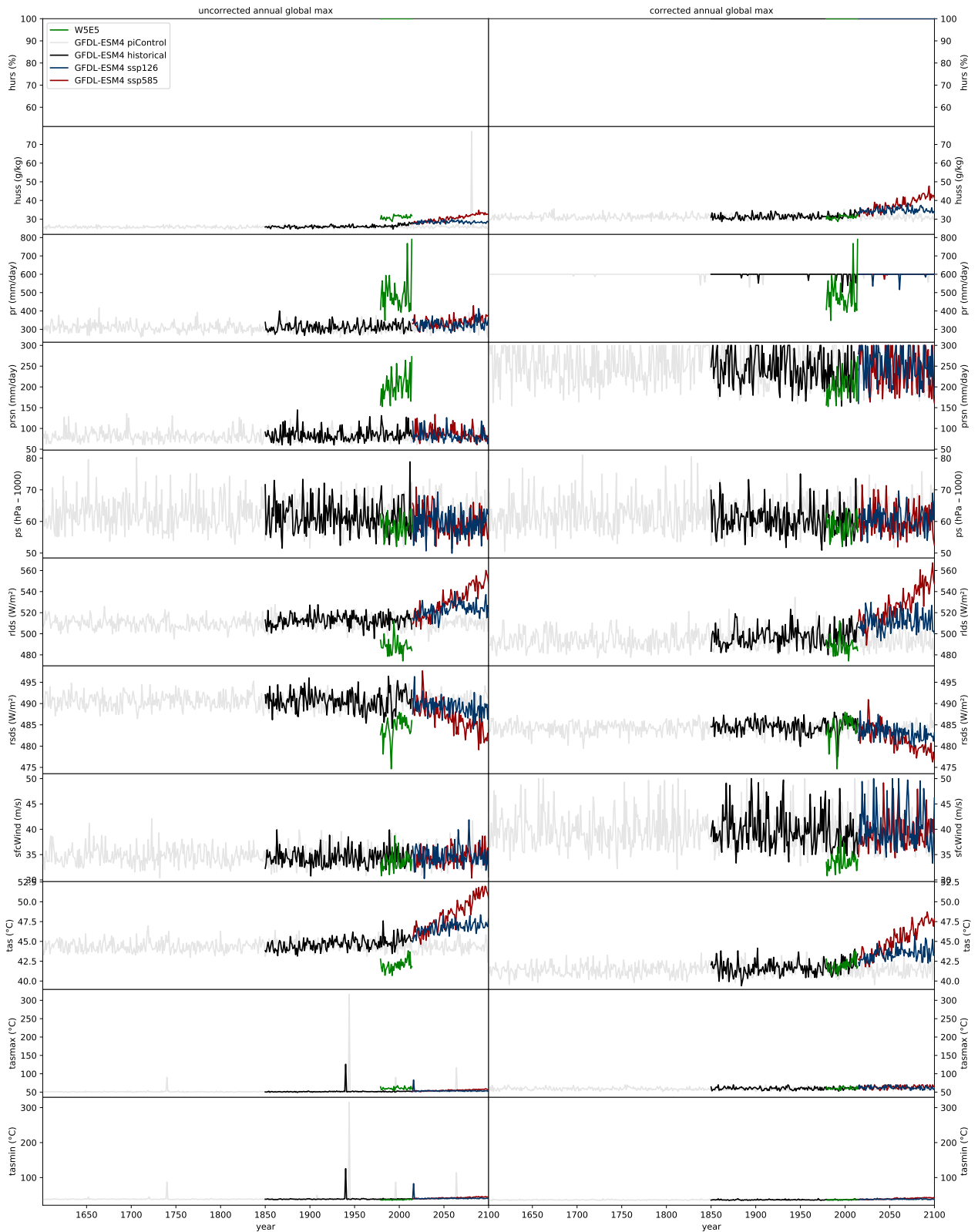


Figure 7: Same as Figure 5 but for annual global maximum values.

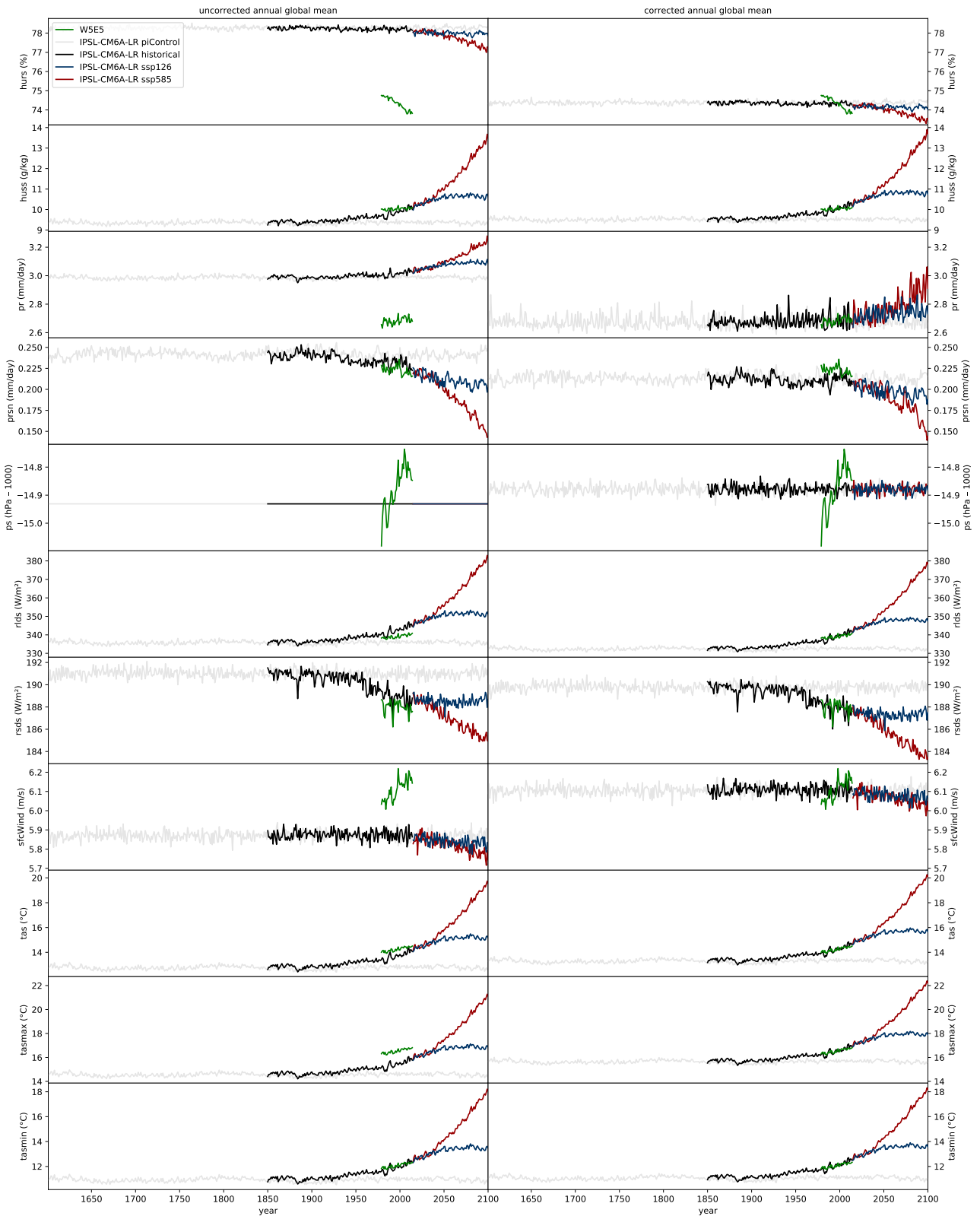


Figure 8: Same as Figure 5 but for IPSL-CM6A-LR.

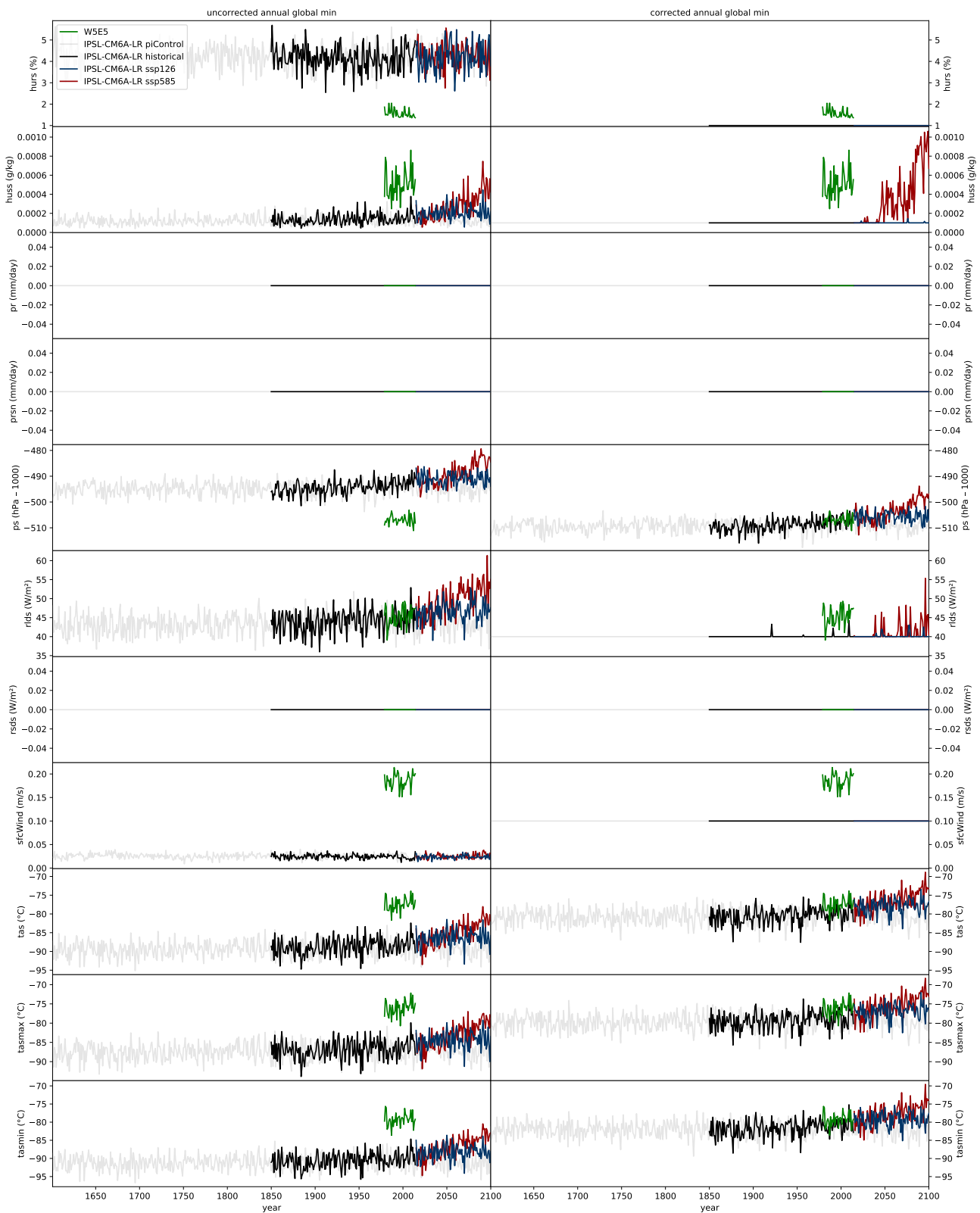


Figure 9: Same as Figure 6 but for IPSL-CM6A-LR.

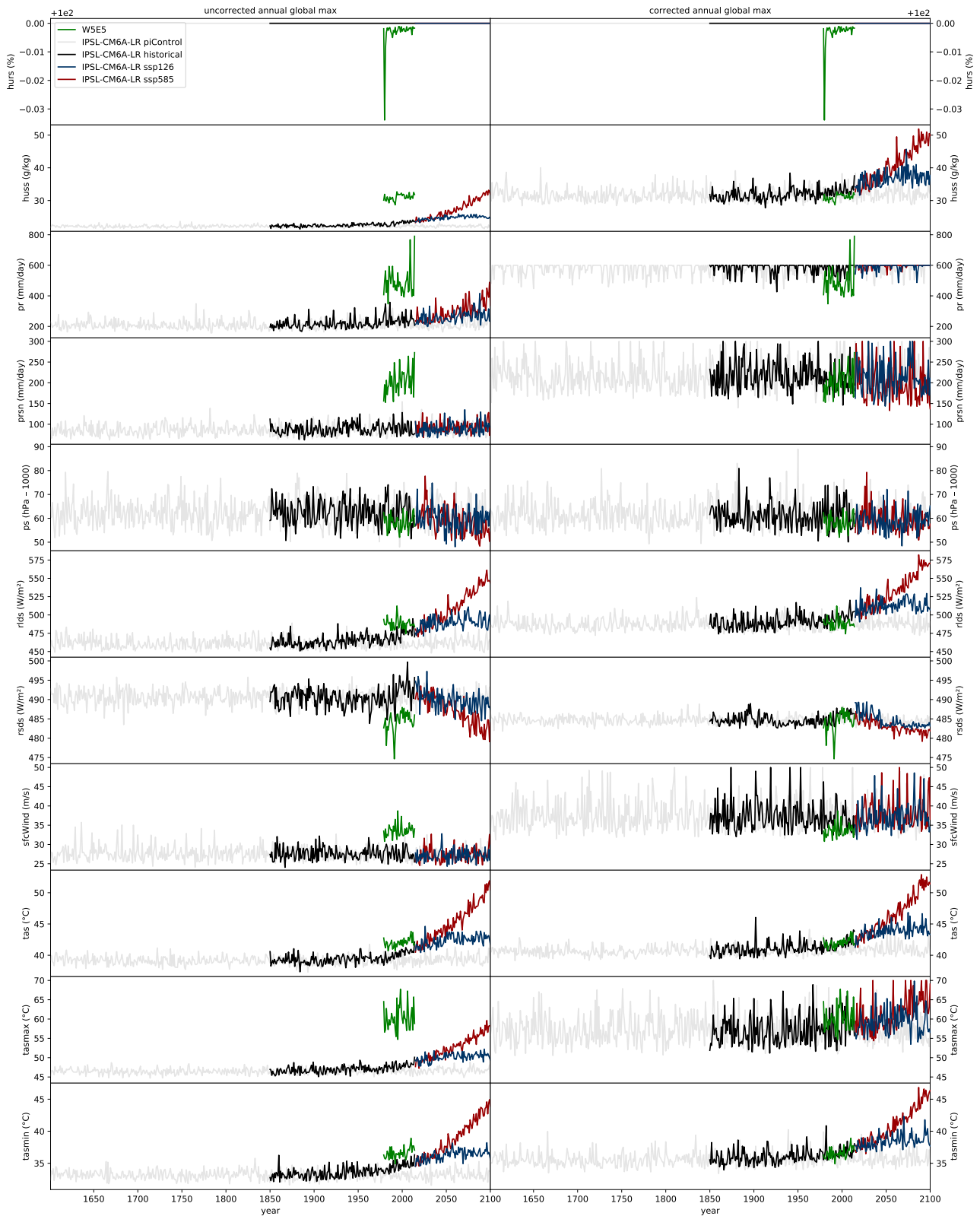


Figure 10: Same as Figure 7 but for IPSL-CM6A-LR.

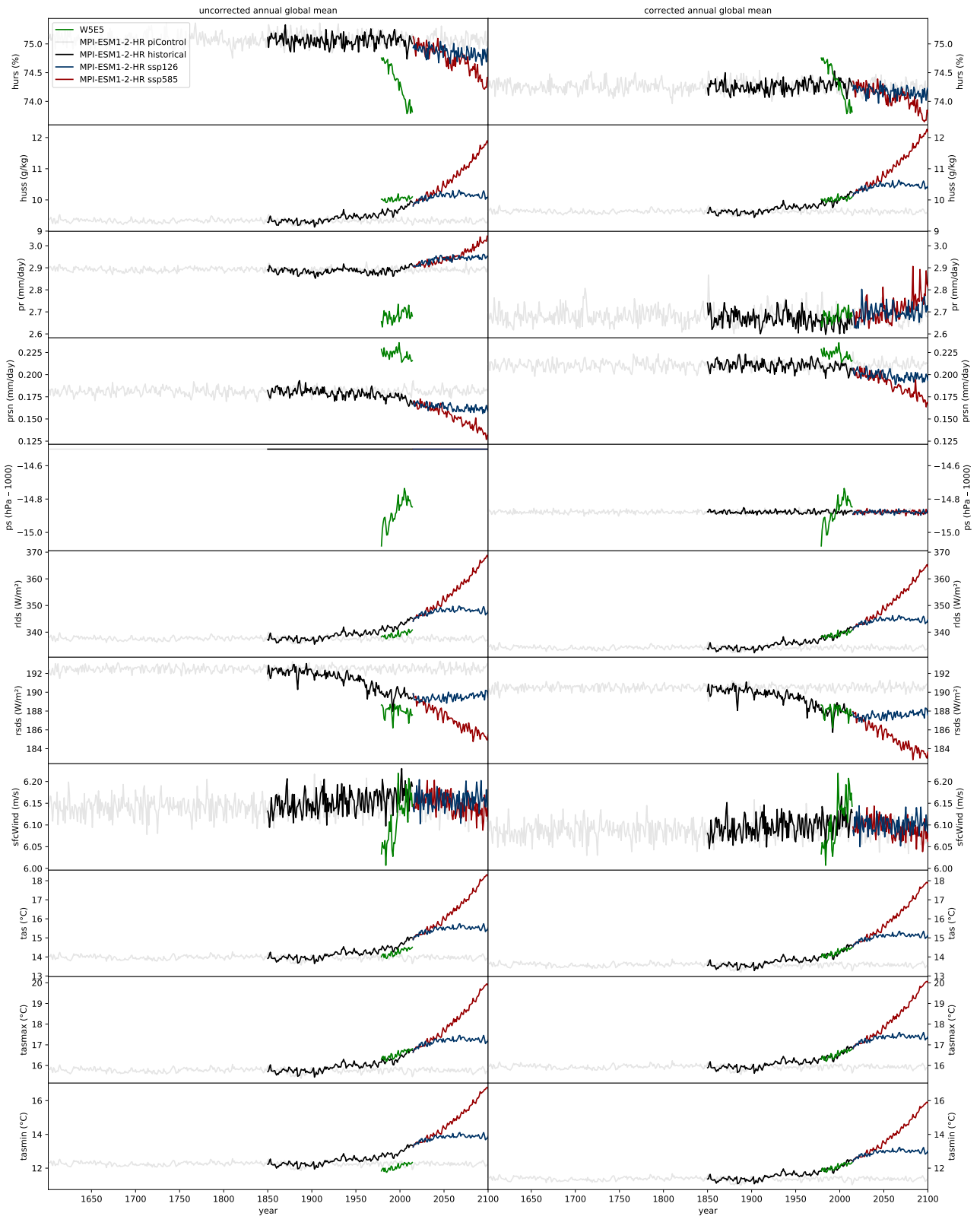


Figure 11: Same as Figure 5 but for MPI-ESM1-2-HR.

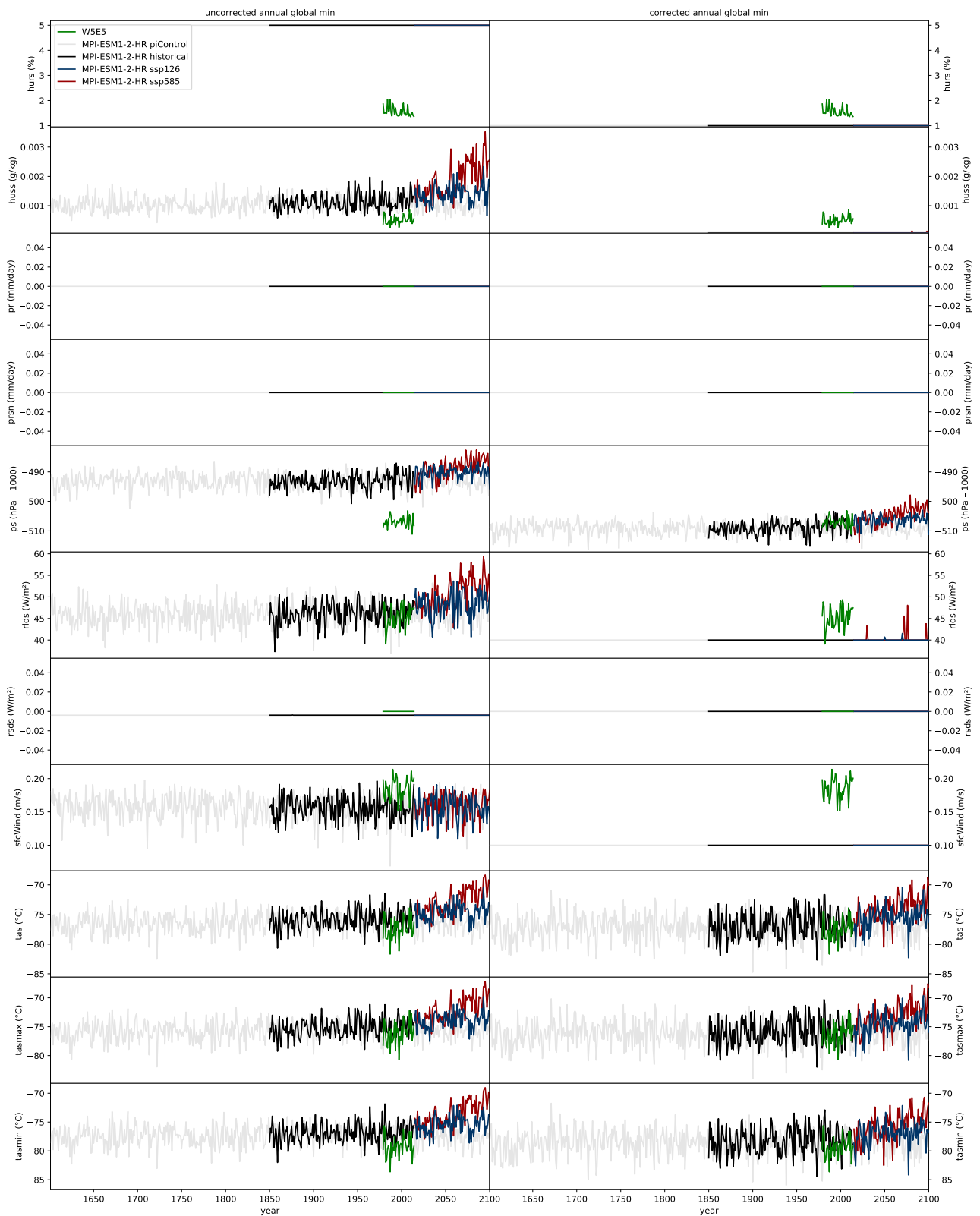


Figure 12: Same as Figure 6 but for MPI-ESM1-2-HR.

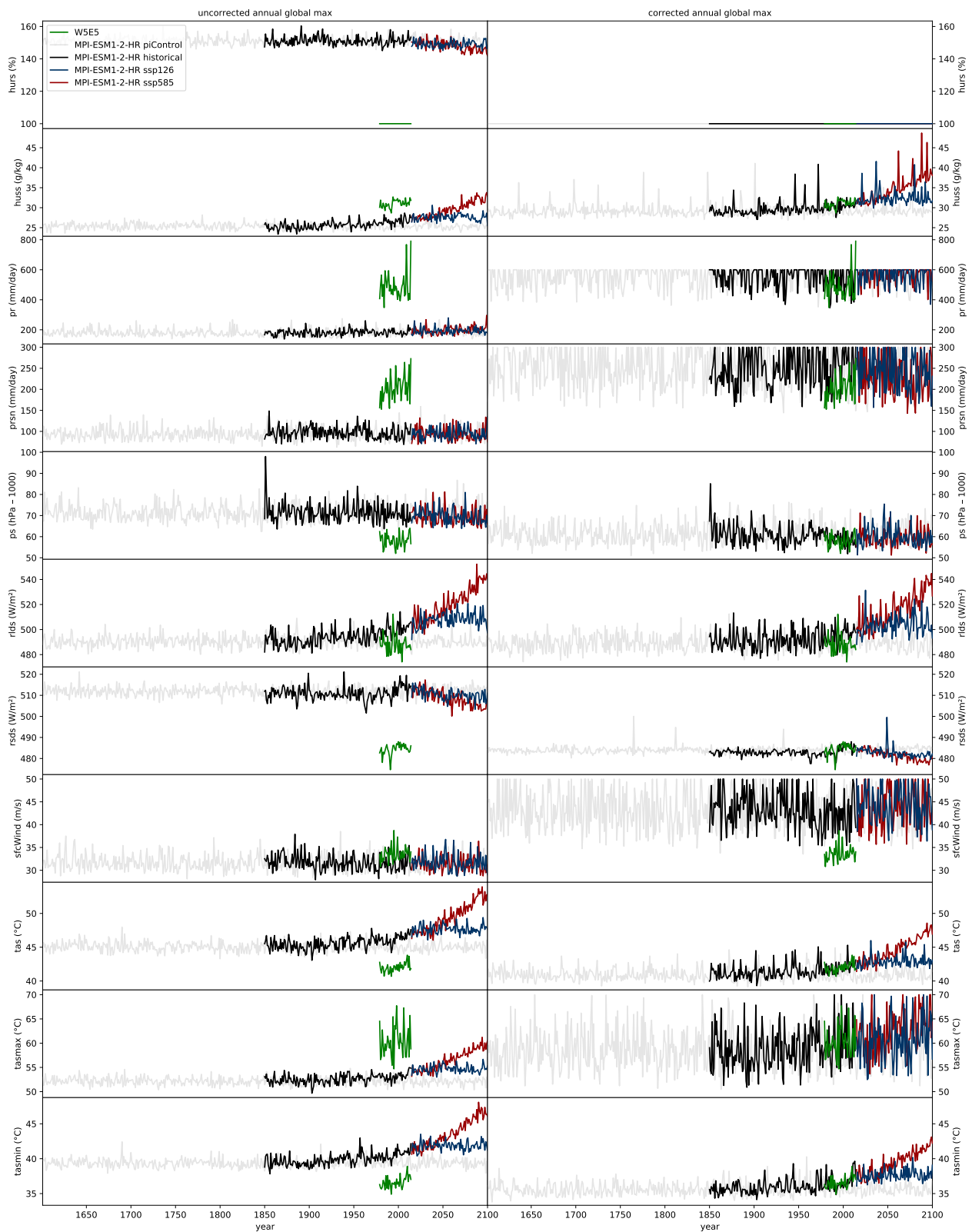


Figure 13: Same as Figure 7 but for MPI-ESM1-2-HR.

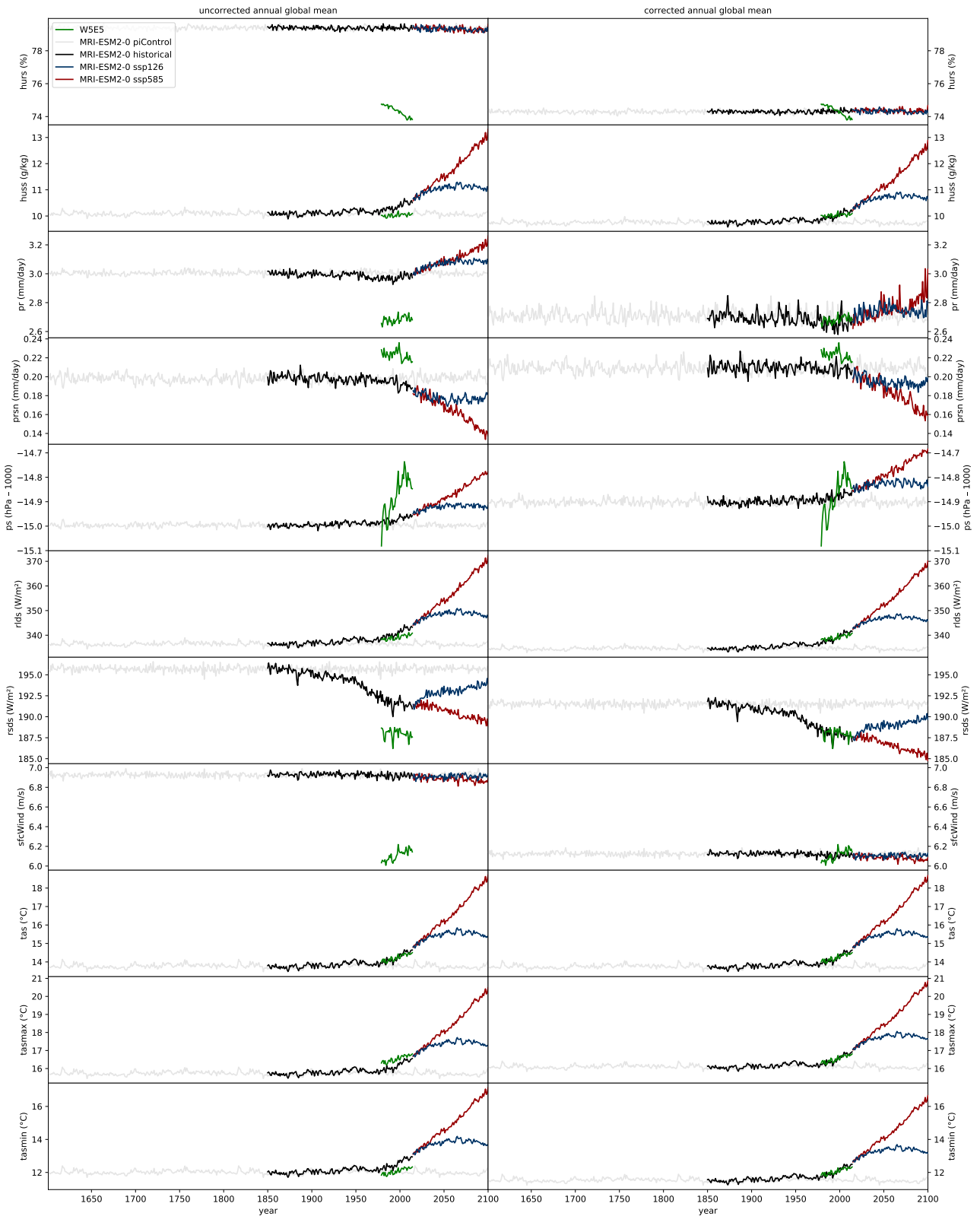


Figure 14: Same as Figure 5 but for MRI-ESM2-0.

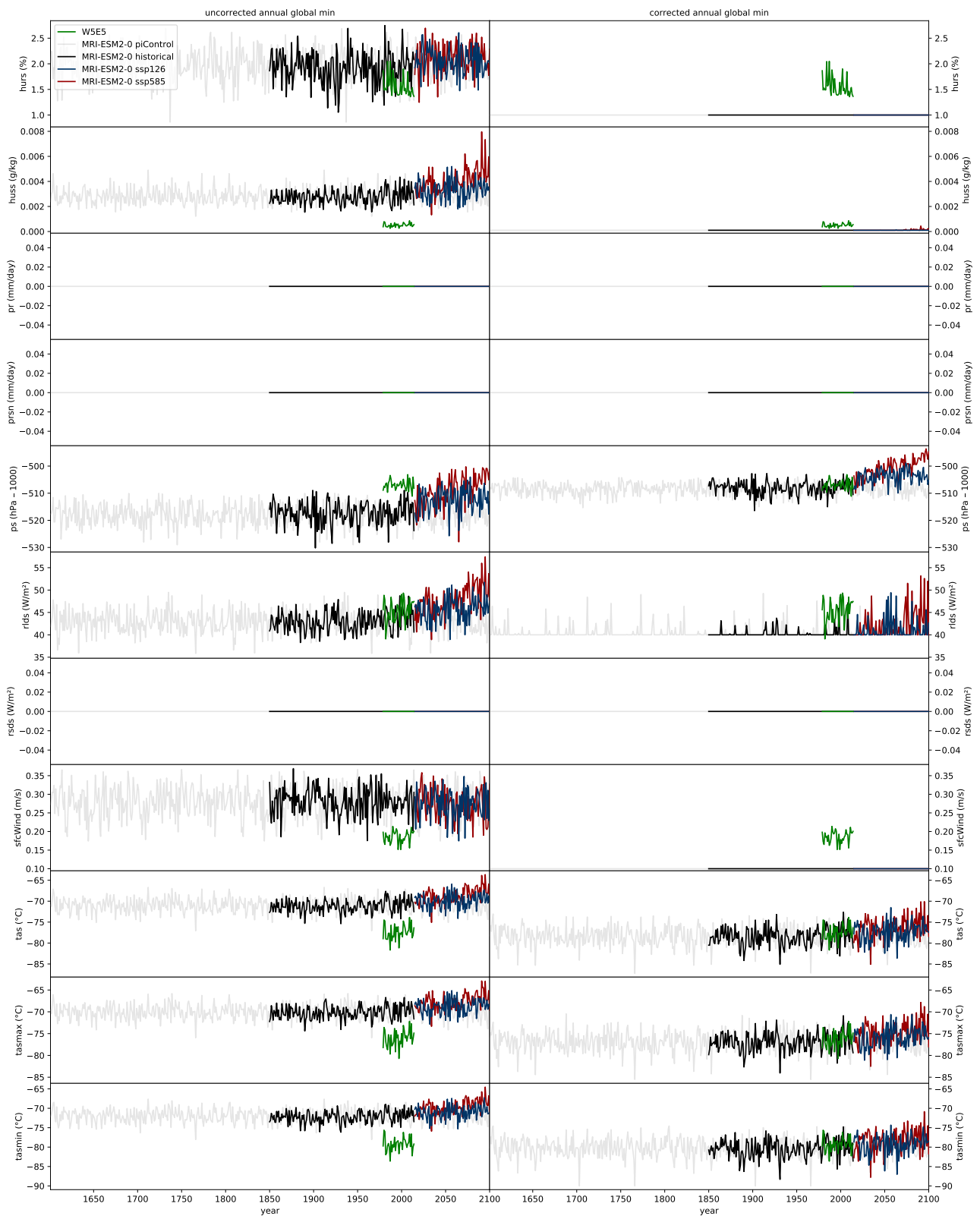


Figure 15: Same as Figure 6 but for MRI-ESM2-0.

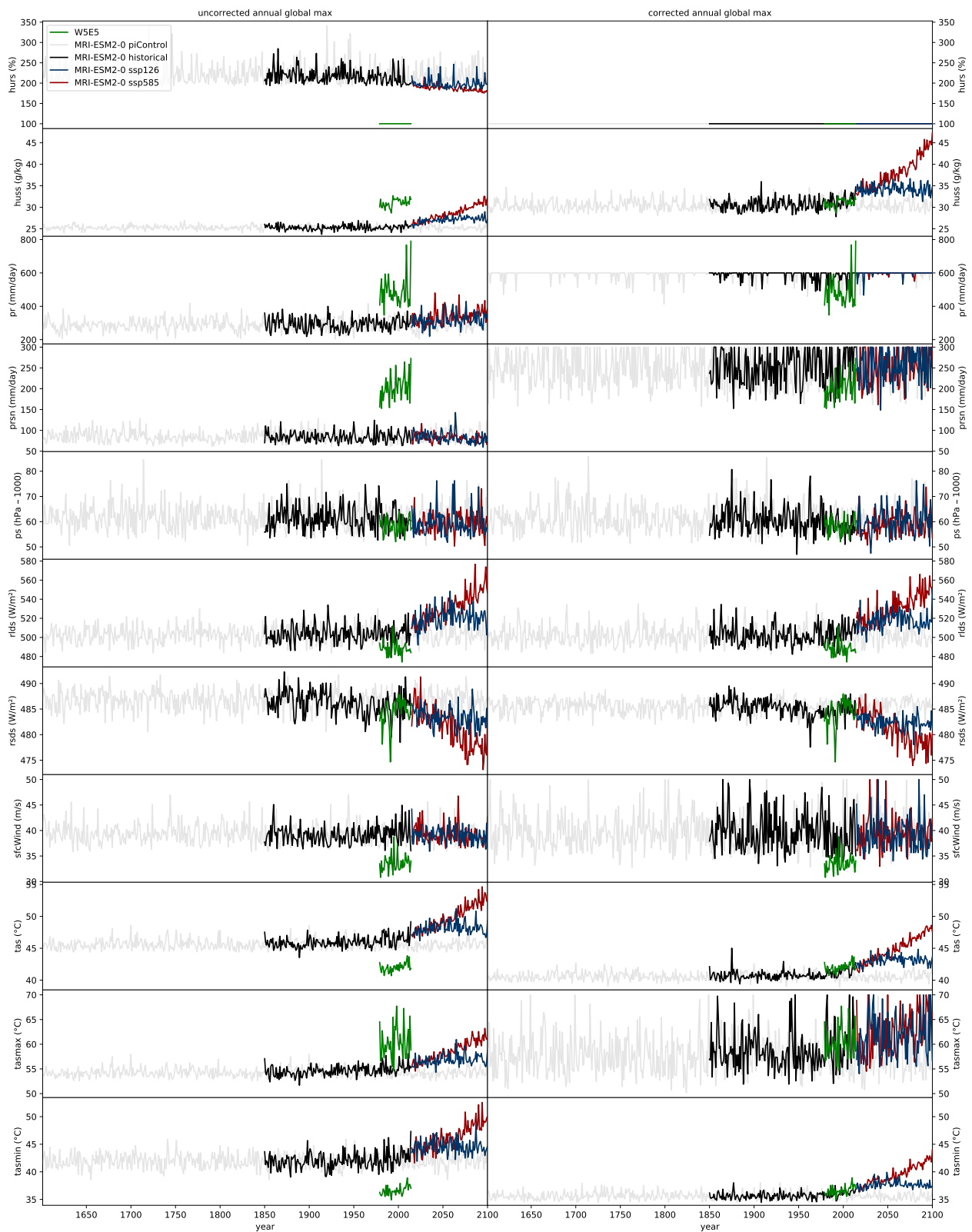


Figure 16: Same as Figure 7 but for MRI-ESM2-0.

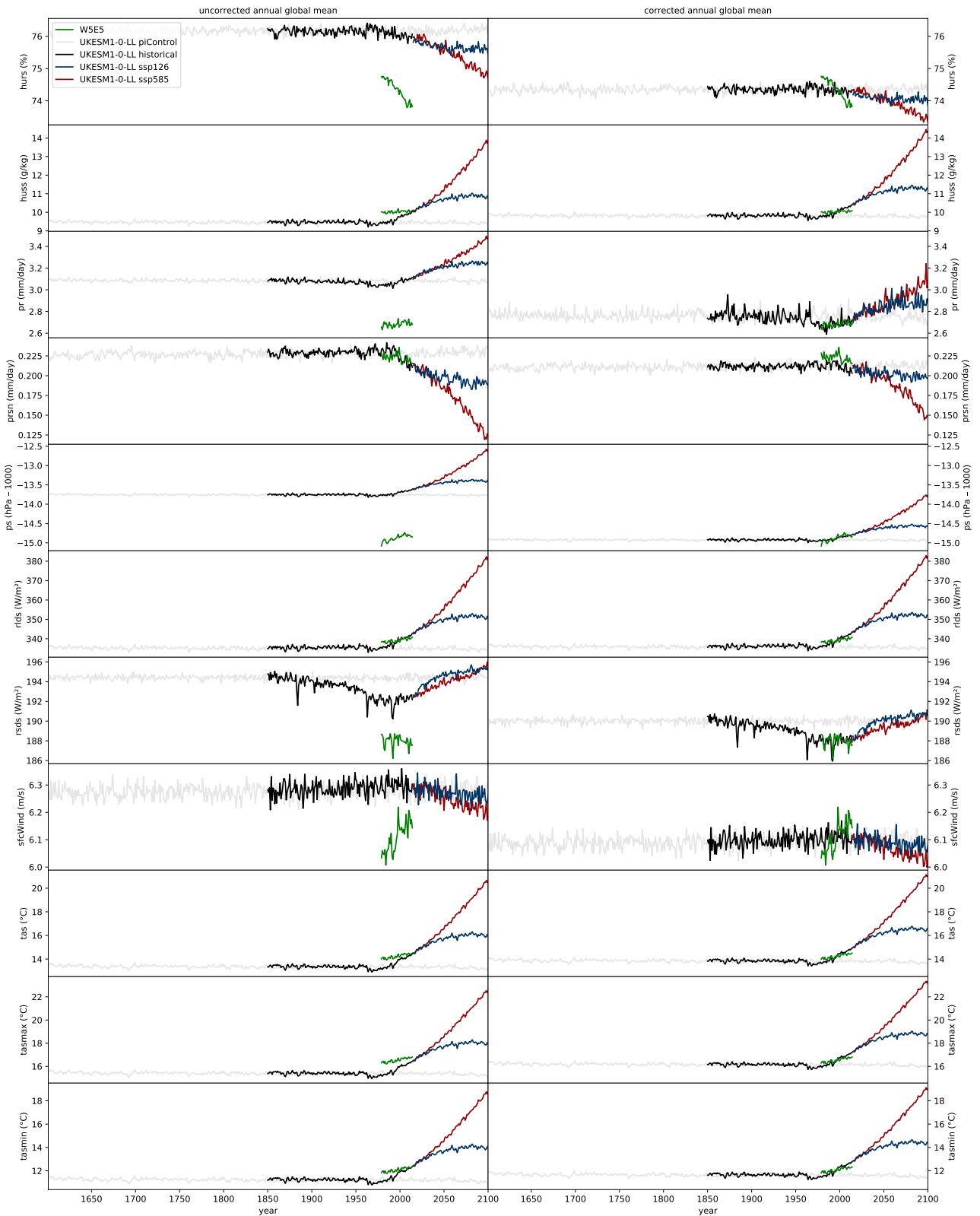


Figure 17: Same as Figure 5 but for UKESM1-0-LL.

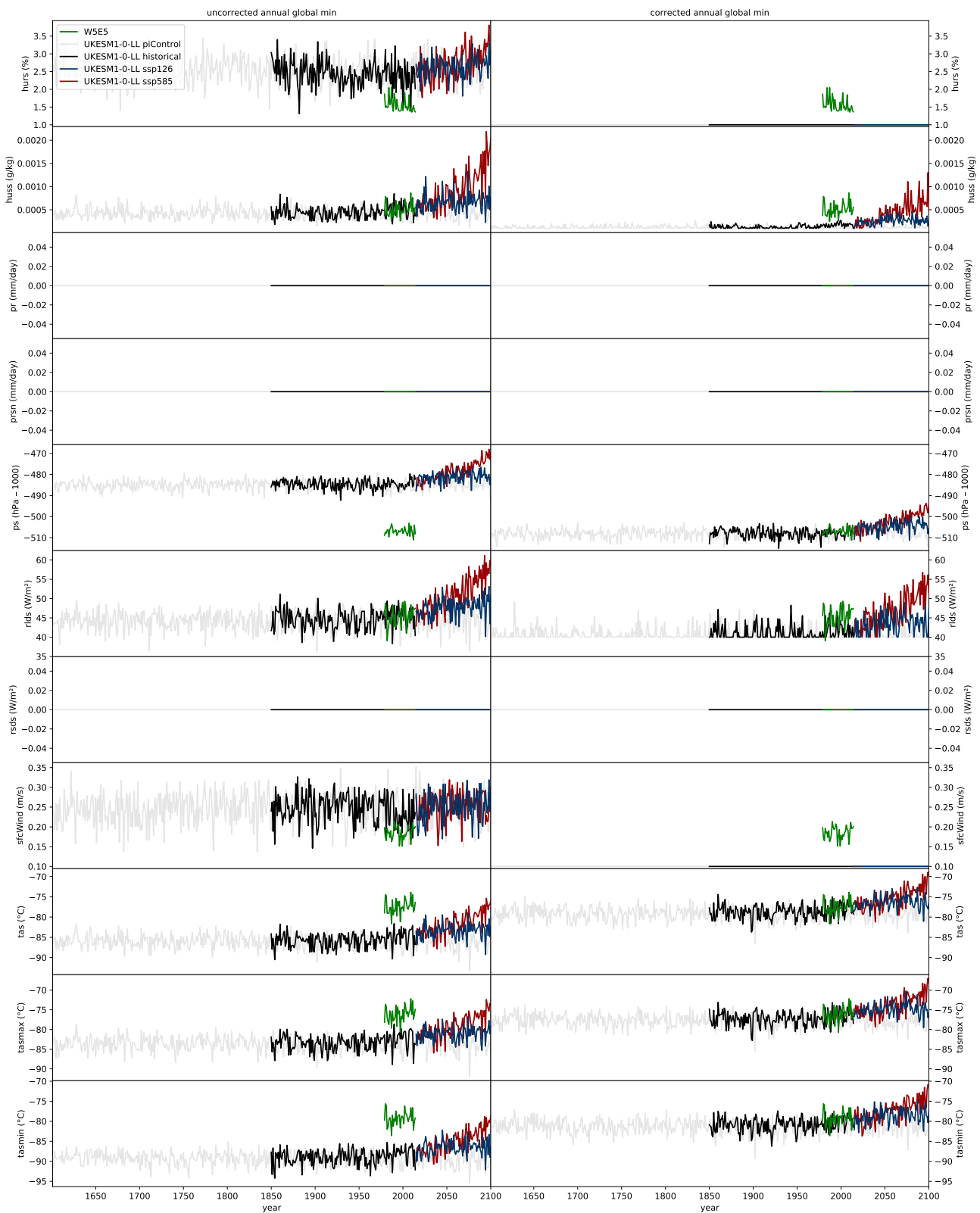


Figure 18: Same as Figure 6 but for UKESM1-0-LL.

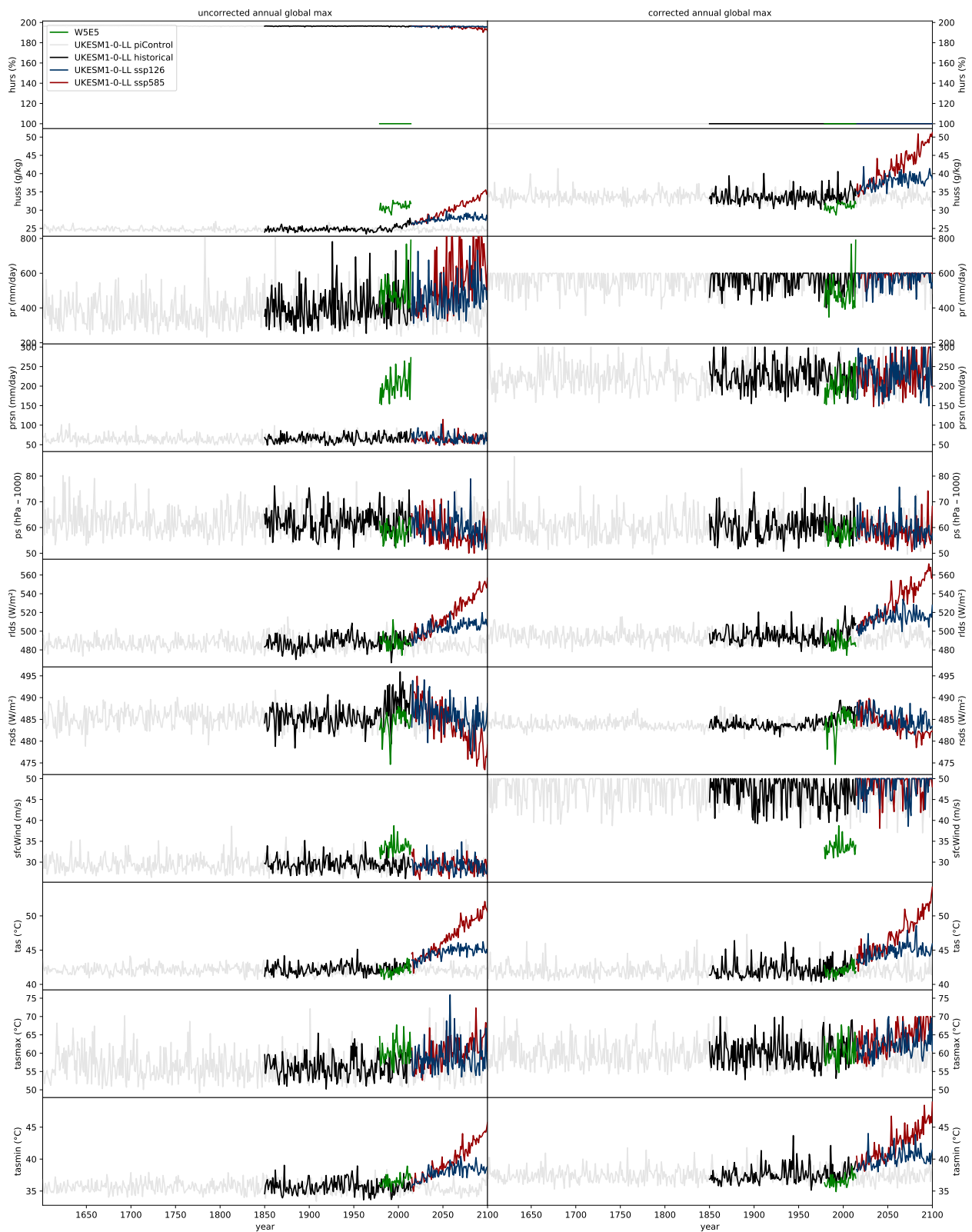


Figure 19: Same as Figure 7 but for UKESM1-0-LL.

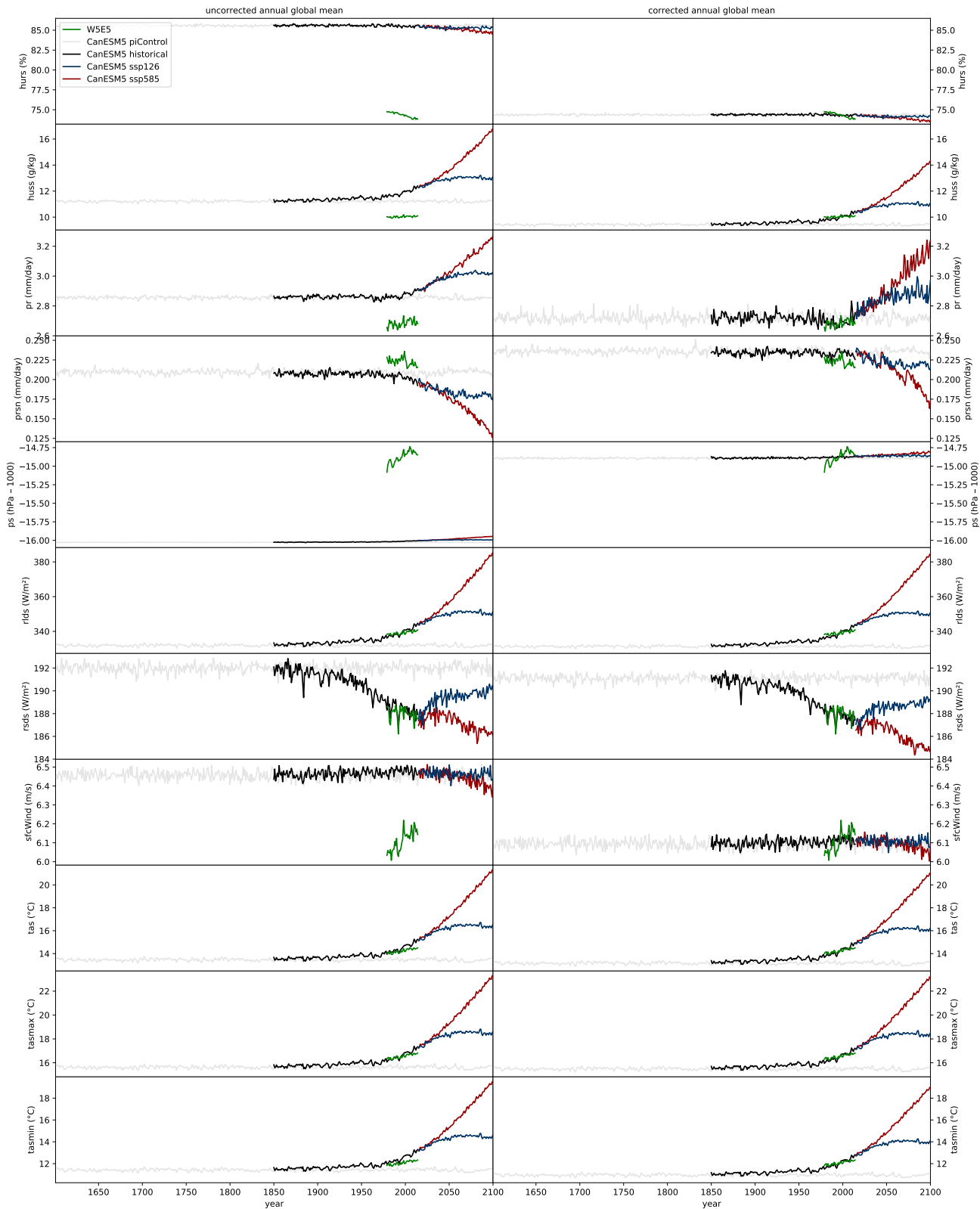


Figure 20: Same as Figure 5 but for CanESM5.

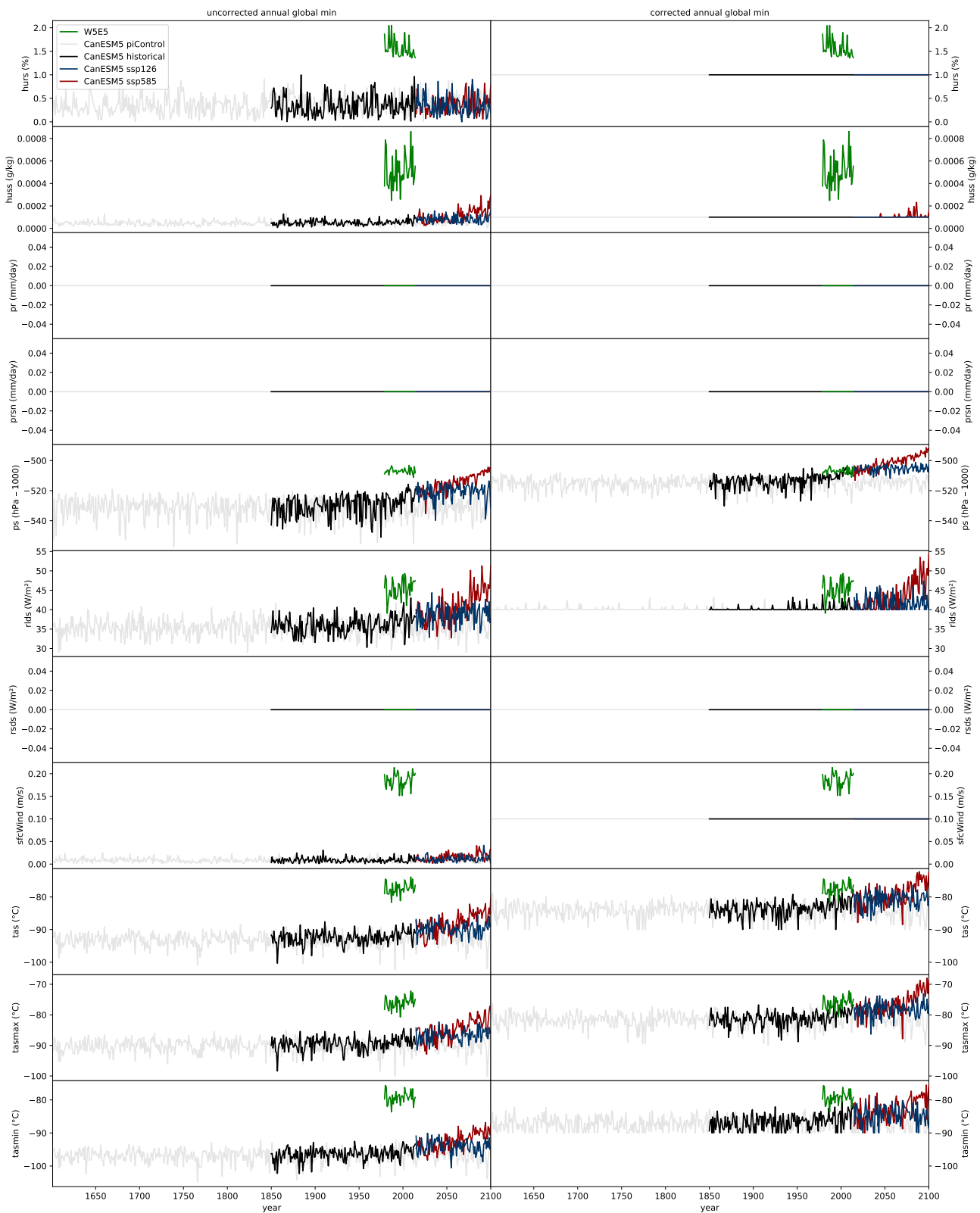


Figure 21: Same as Figure 6 but for CanESM5.

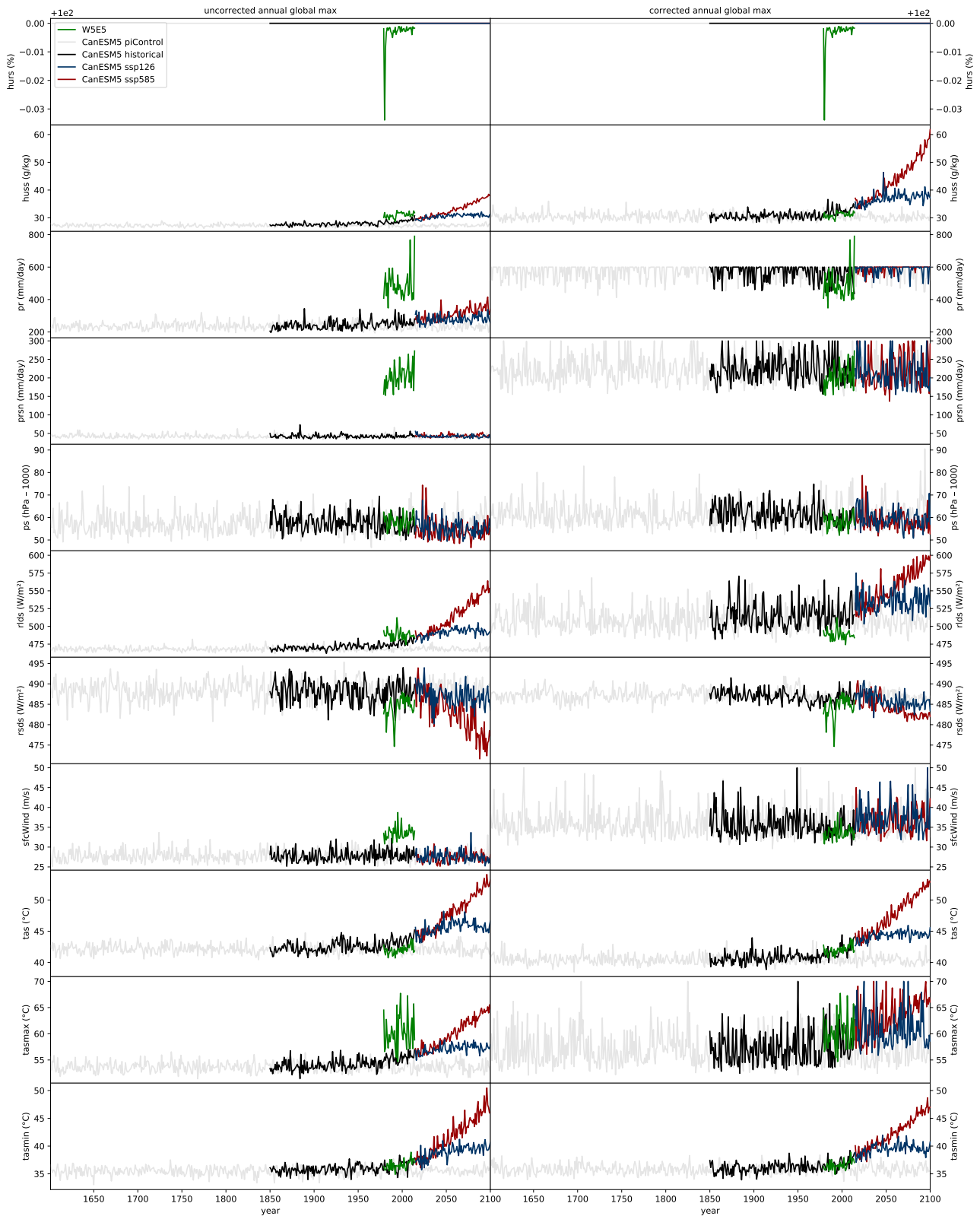


Figure 22: Same as Figure 7 but for CanESM5.

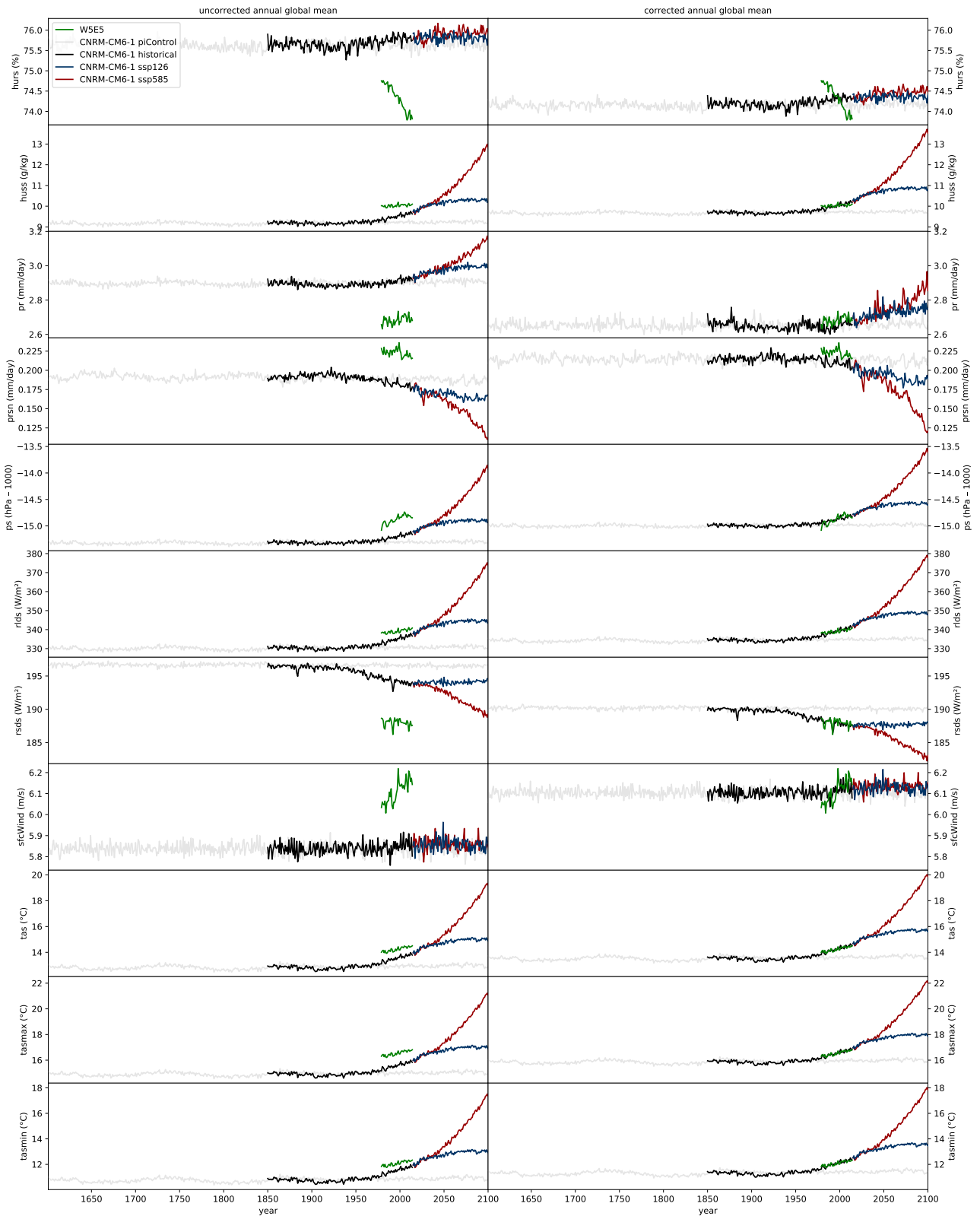


Figure 23: Same as Figure 5 but for CNRM-CM6-1.

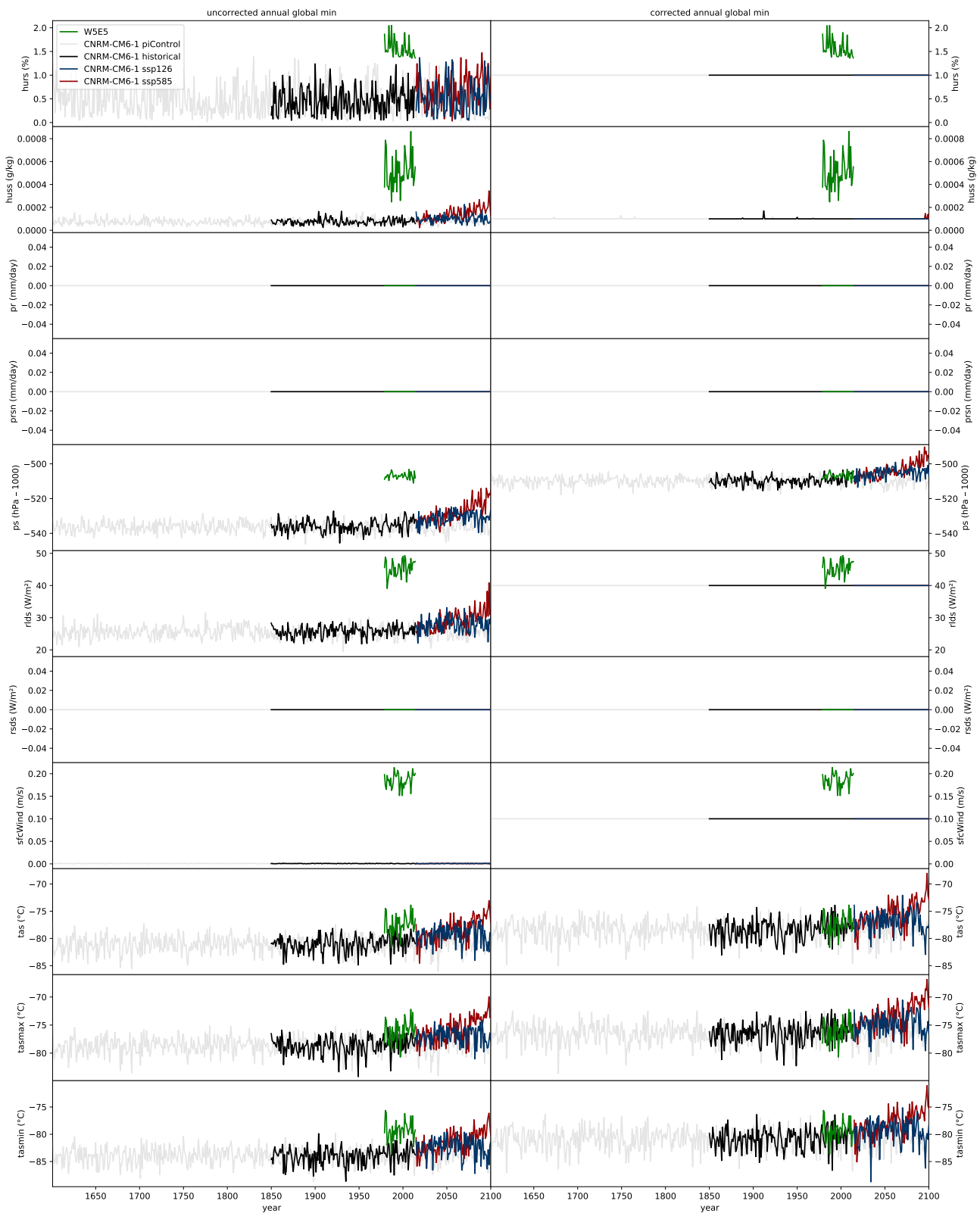


Figure 24: Same as Figure 6 but for CNRM-CM6-1.

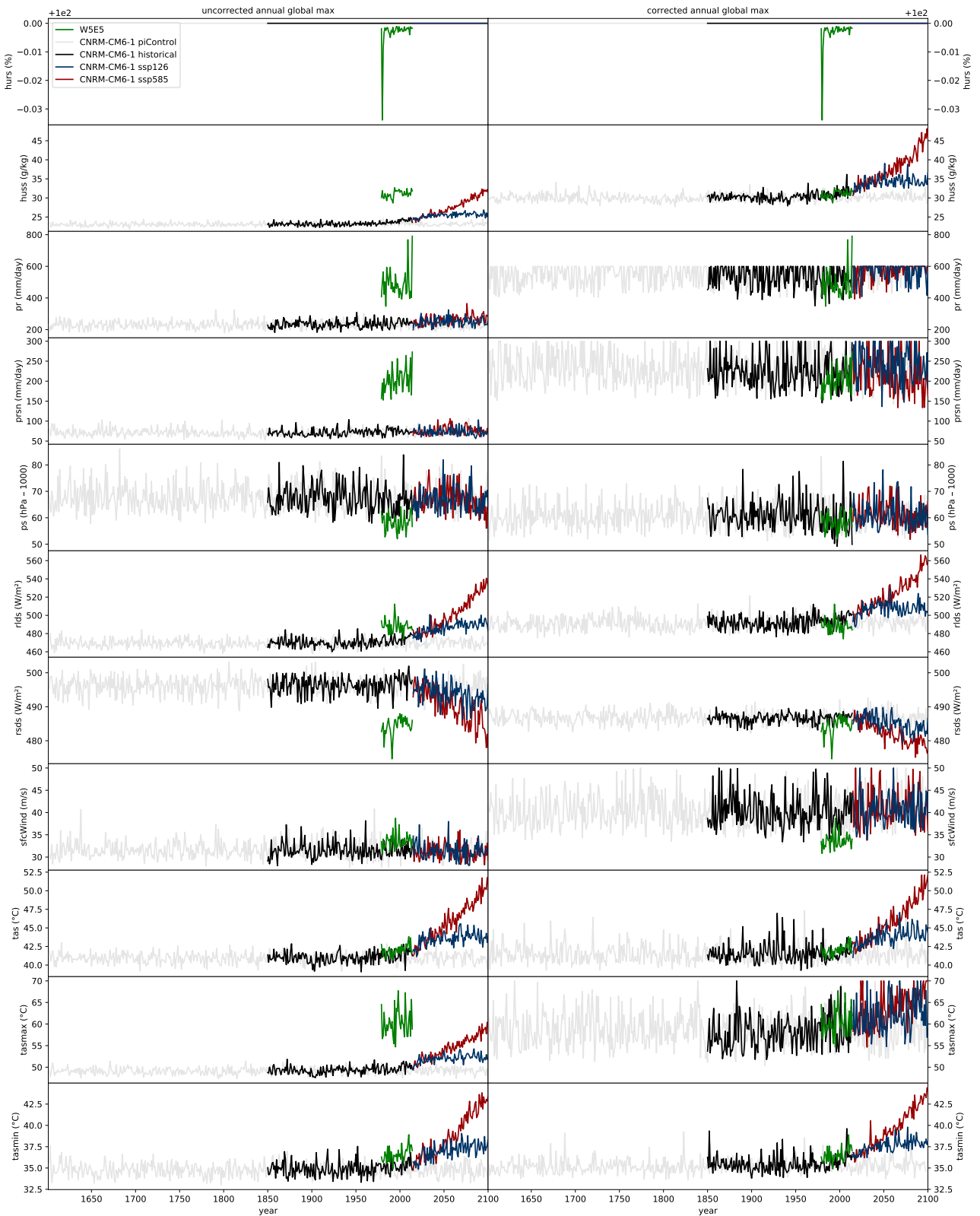


Figure 25: Same as Figure 7 but for CNRM-CM6-1.

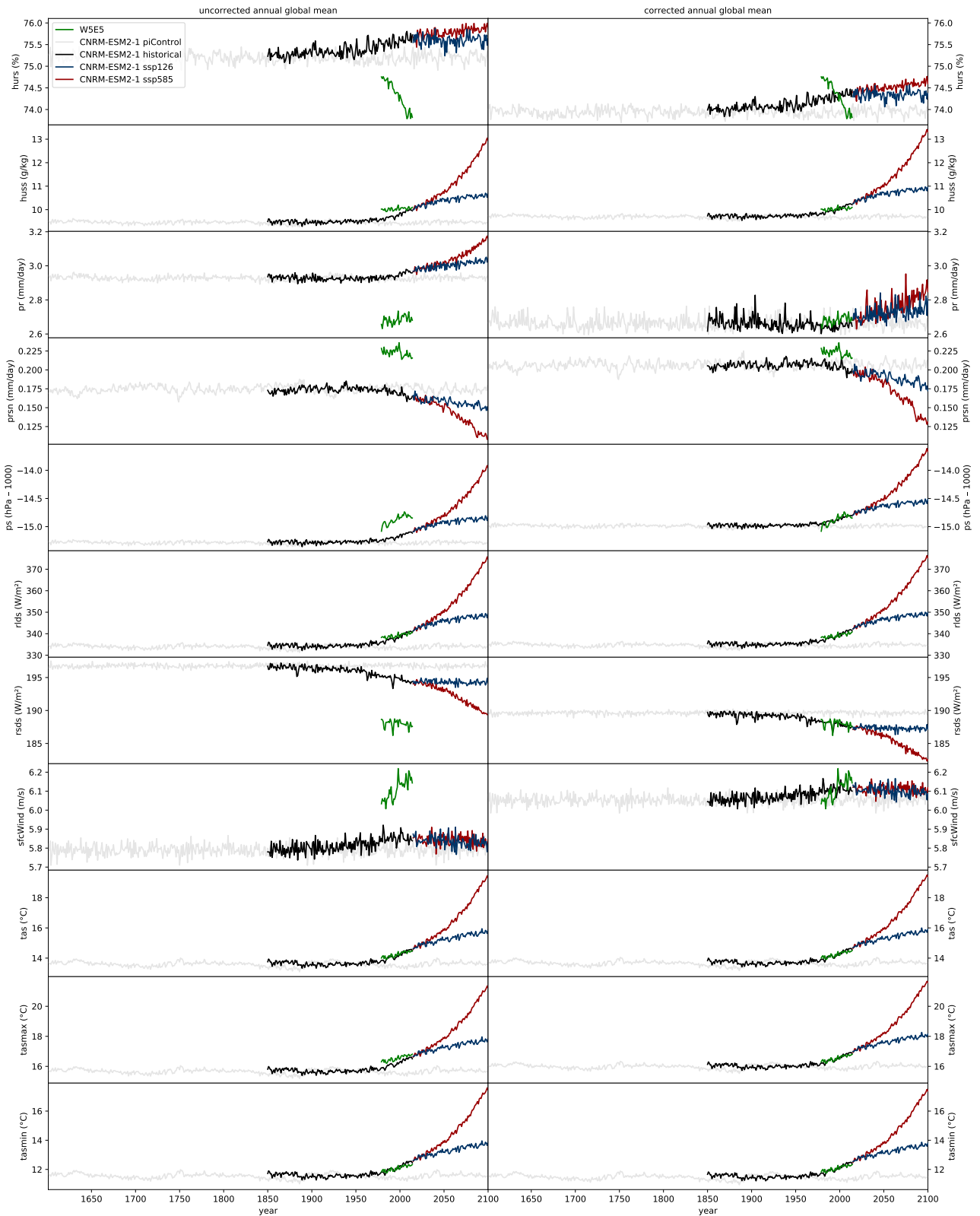


Figure 26: Same as Figure 5 but for CNRM-ESM2-1.

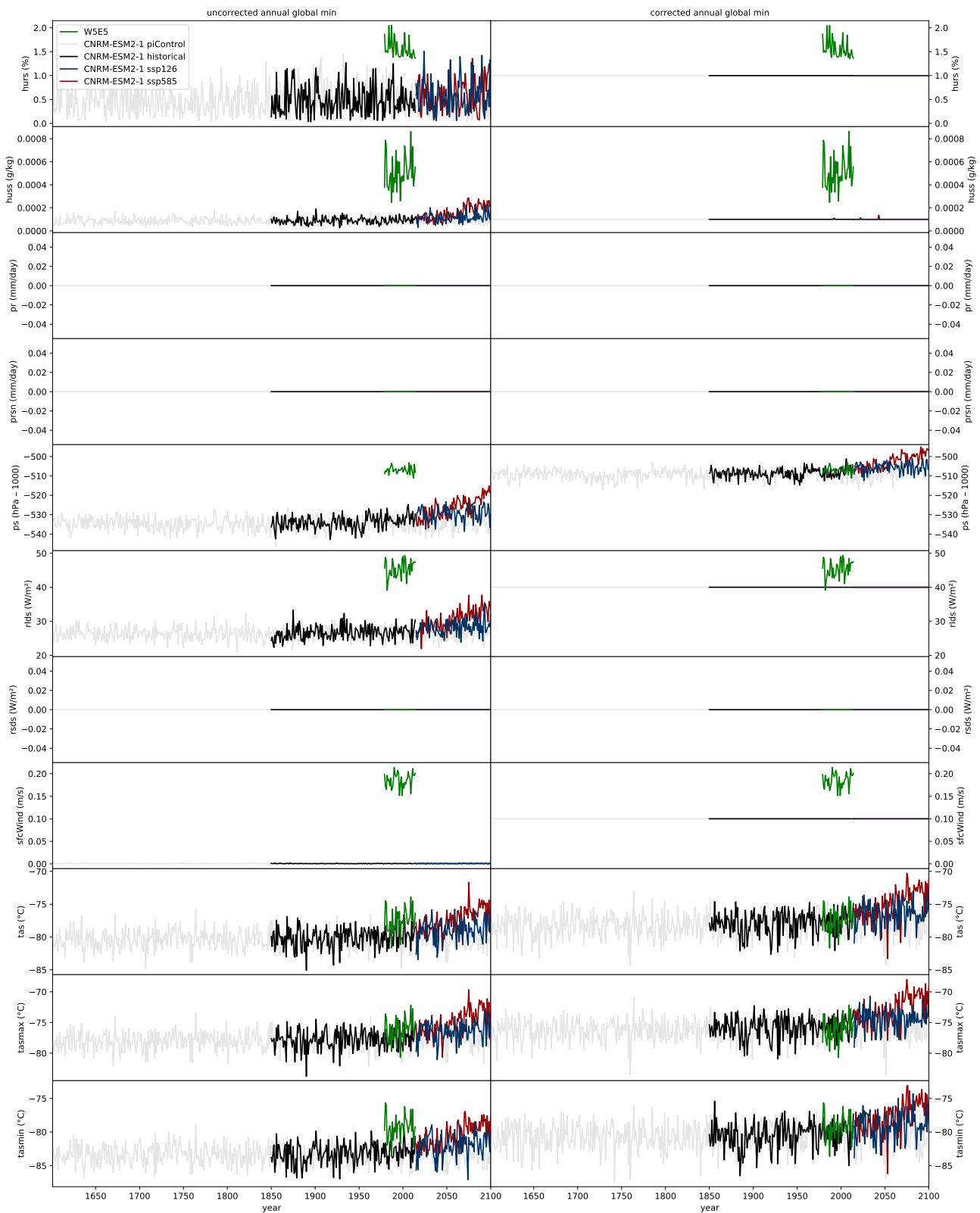


Figure 27: Same as Figure 6 but for CNRM-ESM2-1.

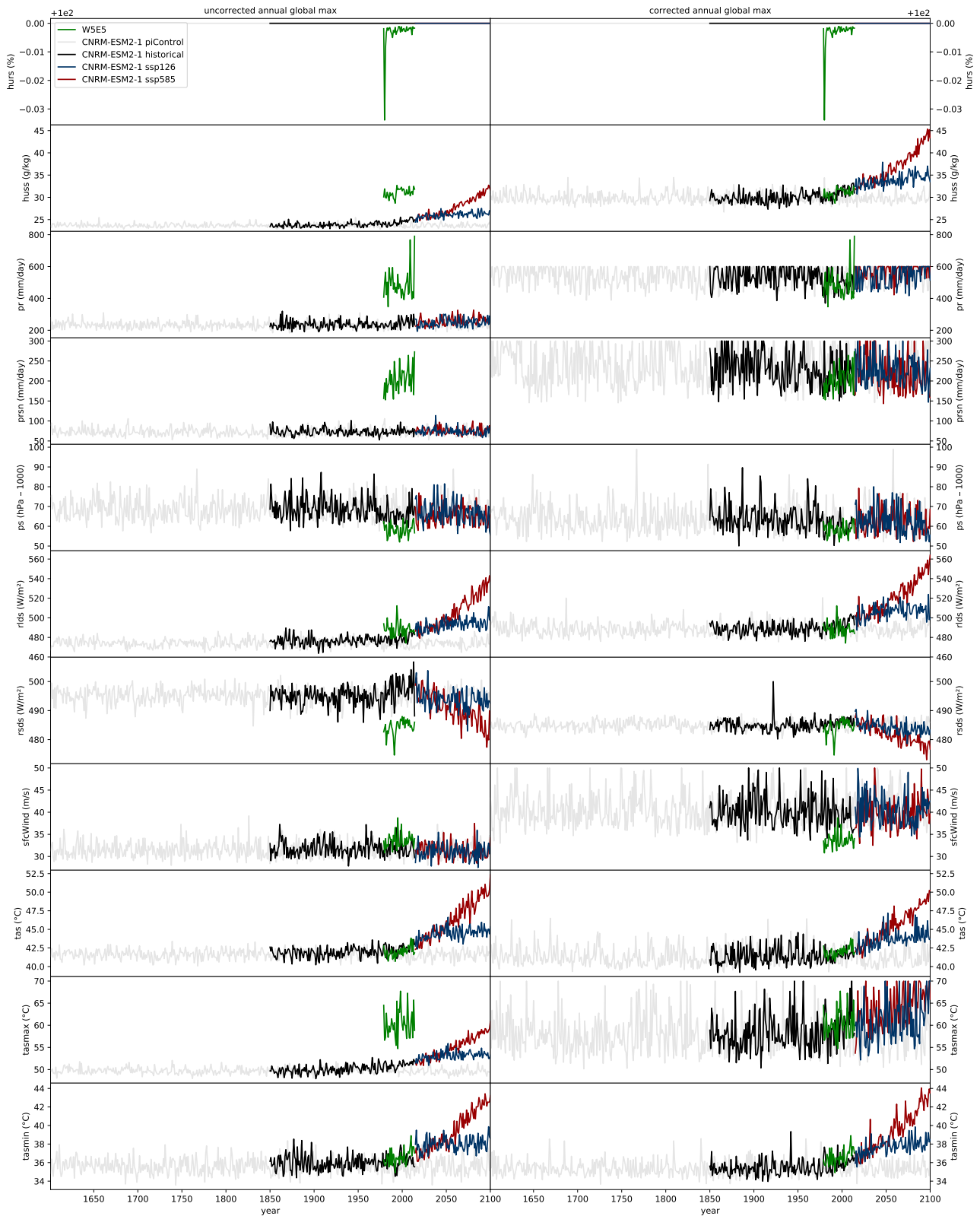


Figure 28: Same as Figure 7 but for CNRM-ESM2-1.

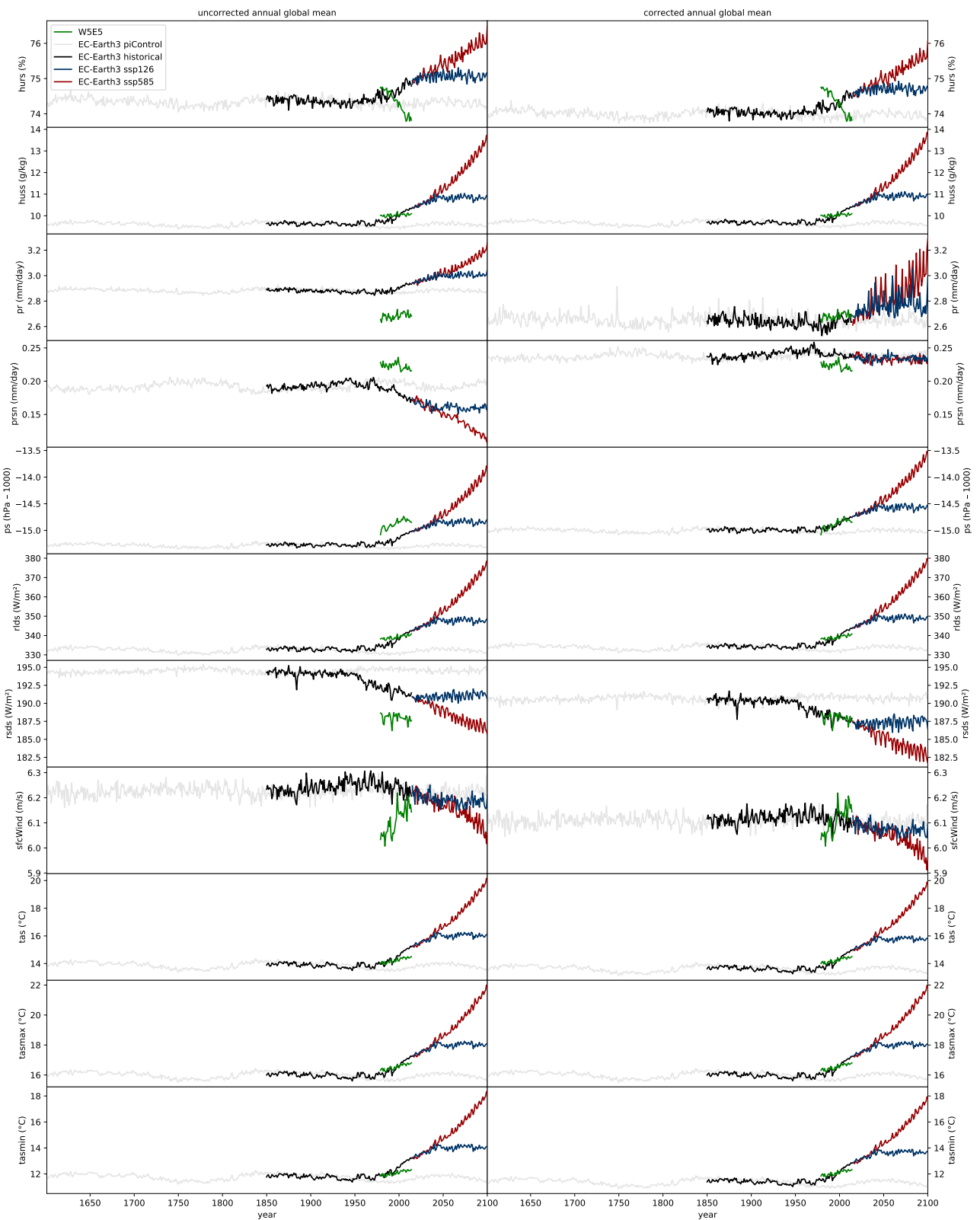


Figure 29: Same as Figure 5 but for EC-Earth3.

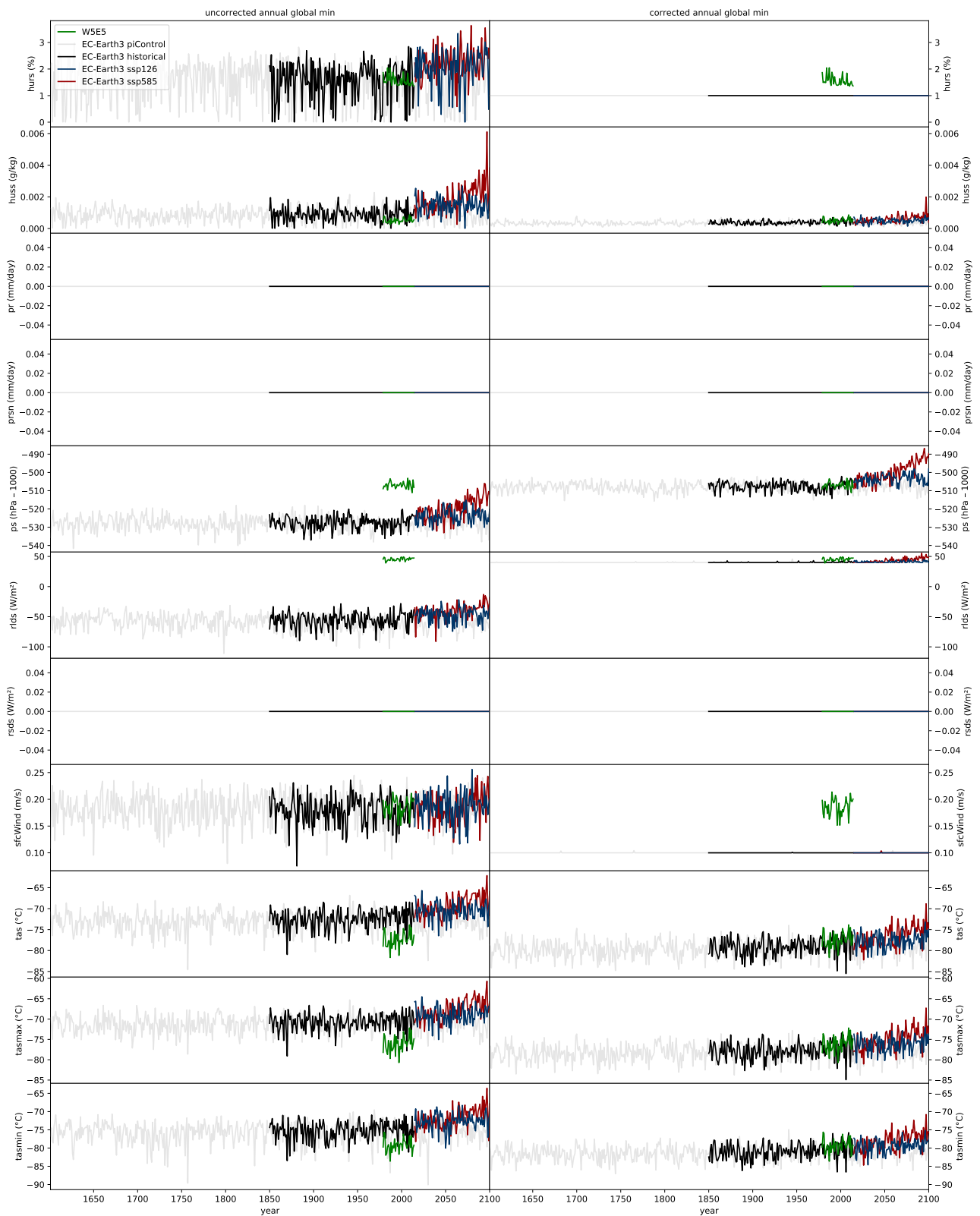


Figure 30: Same as Figure 6 but for EC-Earth3.

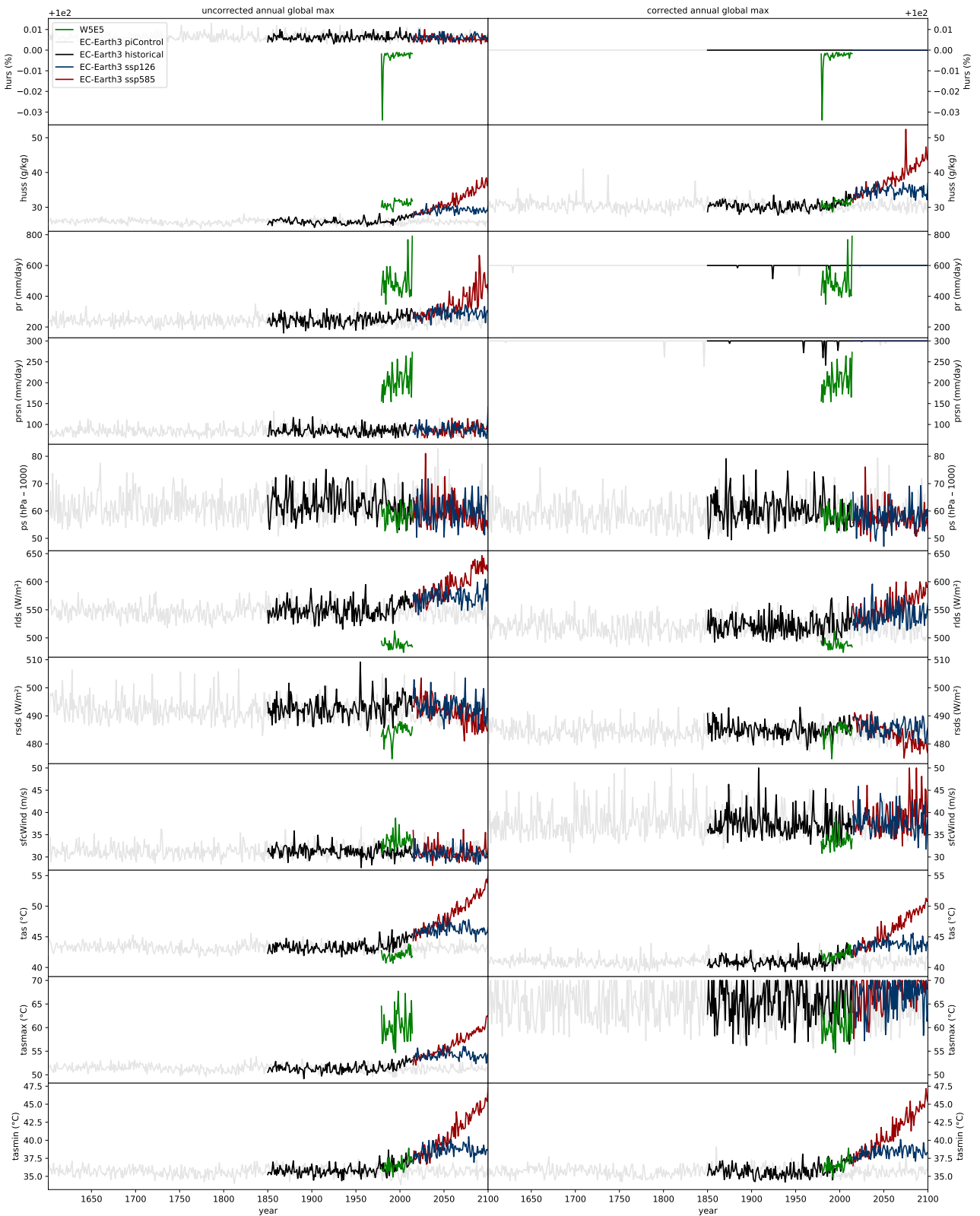


Figure 31: Same as Figure 7 but for EC-Earth3.

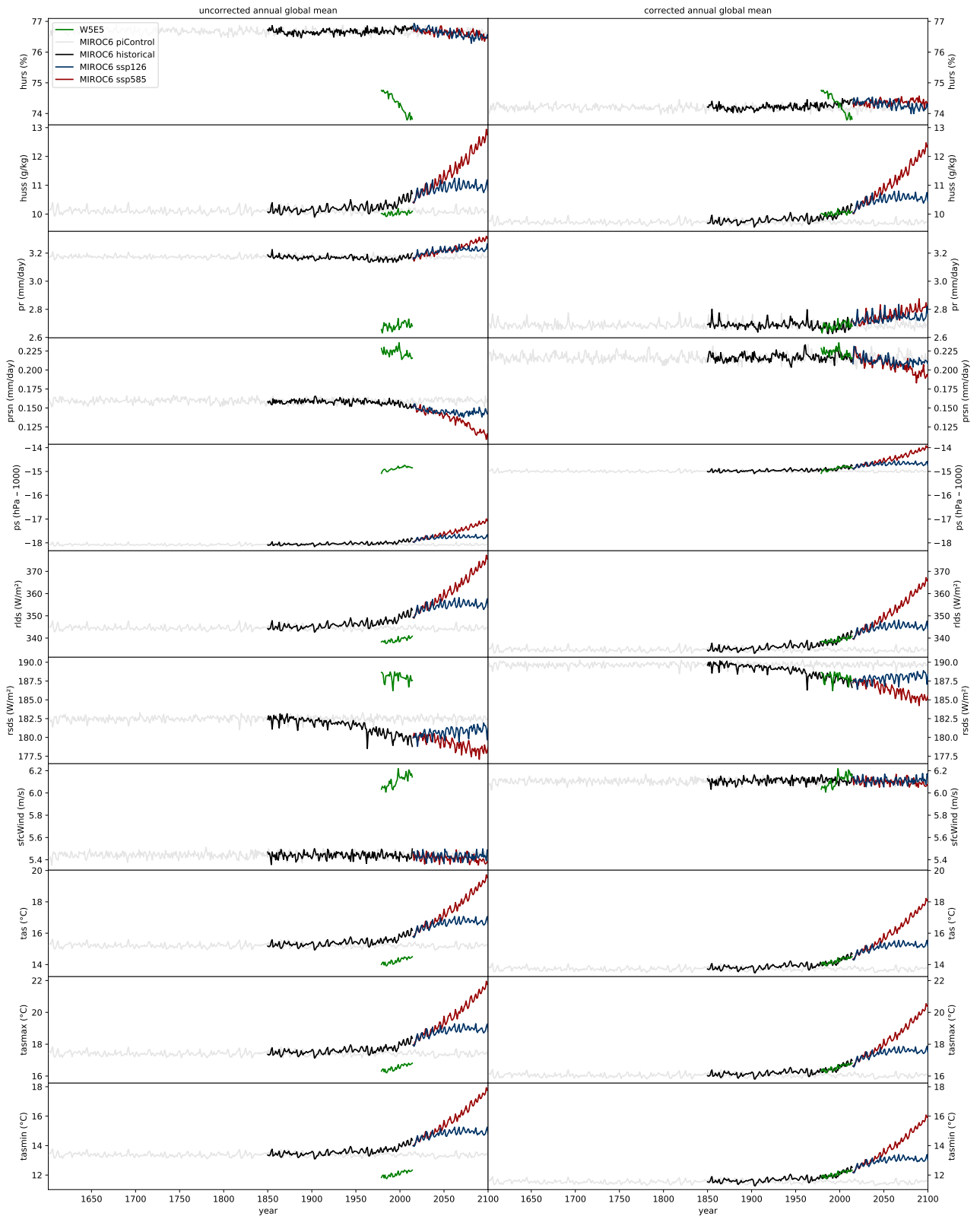


Figure 32: Same as Figure 5 but for MIROC6.

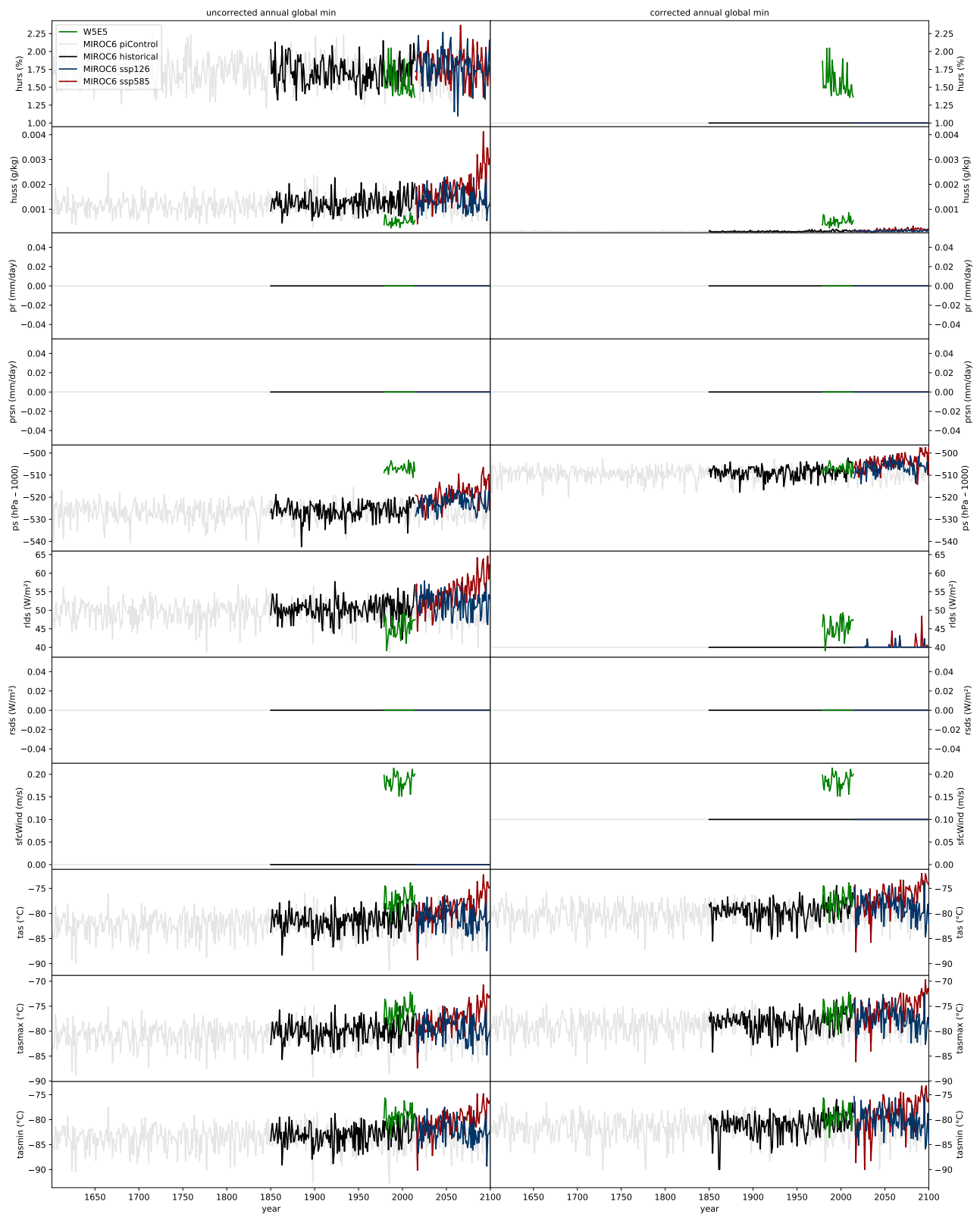


Figure 33: Same as Figure 6 but for MIROC6.

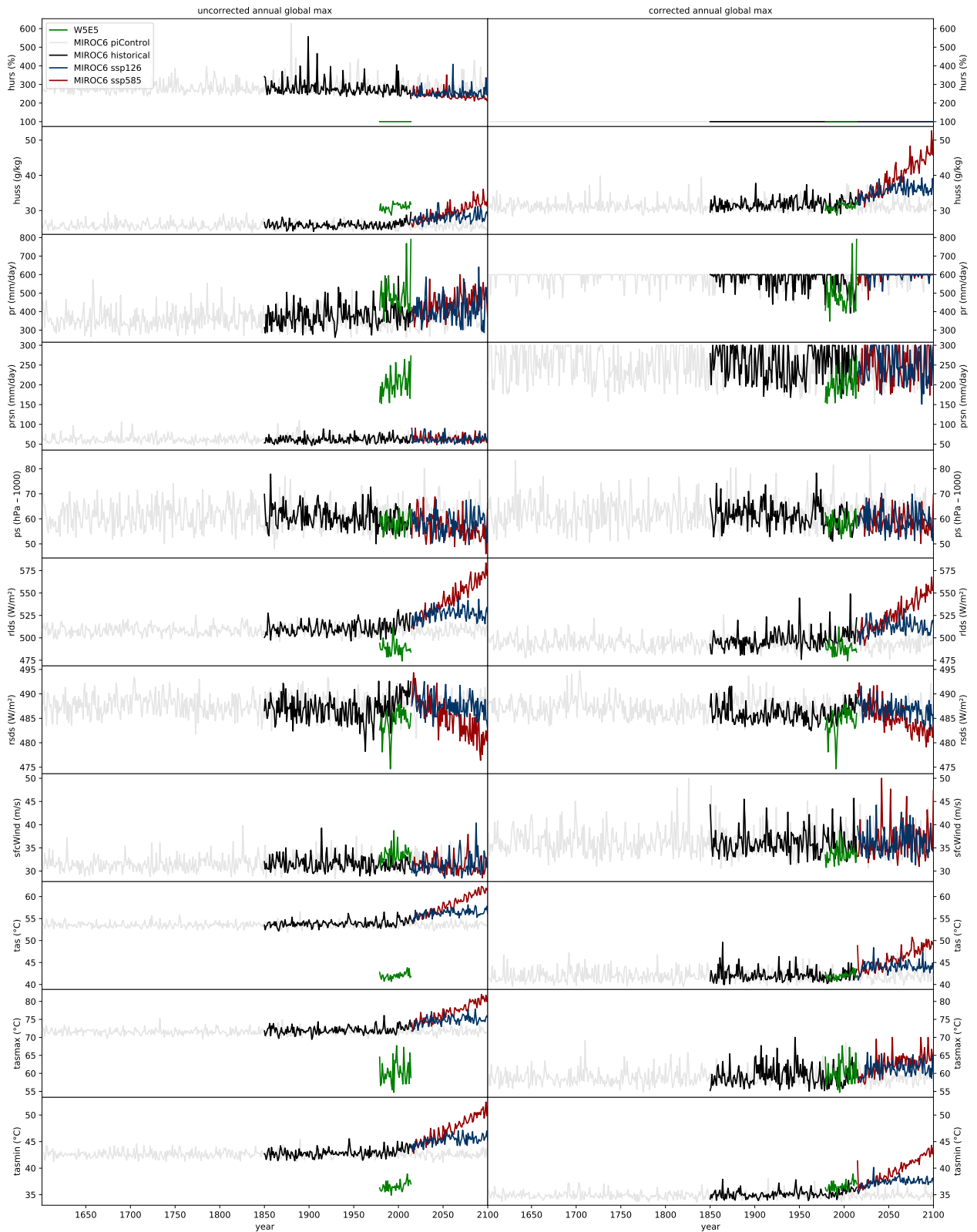


Figure 34: Same as Figure 7 but for MIROC6.

References

- Adler, R. F., Huffman, G. J., Chang, A., Ferraro, R., Xie, P.-P., Janowiak, J., Rudolf, B., Schneider, U., Curtis, S., Bolvin, D., Gruber, A., Susskind, J., Arkin, P., and Nelkin, E.: The Version-2 Global Precipitation Climatology Project (GPCP) Monthly Precipitation Analysis (1979–Present), *Journal of Hydrometeorology*, 4, 1147–1167, [https://doi.org/10.1175/1525-7541\(2003\)004<1147:TVGPCP>2.0.CO;2](https://doi.org/10.1175/1525-7541(2003)004<1147:TVGPCP>2.0.CO;2), 2003.
- Cannon, A. J.: Multivariate quantile mapping bias correction: an N-dimensional probability density function transform for climate model simulations of multiple variables, *Climate Dynamics*, pp. 1–19, <https://doi.org/10.1007/s00382-017-3580-6>, 2017.
- Cucchi, M., Weedon, G. P., Amici, A., Bellouin, N., Lange, S., Müller Schmied, H., Hersbach, H., and Buontempo, C.: WFDE5: bias adjusted ERA5 reanalysis data for impact studies, in preparation, 2020.
- Eyring, V., Bony, S., Meehl, G. A., Senior, C. A., Stevens, B., Stouffer, R. J., and Taylor, K. E.: Overview of the Coupled Model Intercomparison Project Phase 6 (CMIP6) experimental design and organization, *Geoscientific Model Development*, 9, 1937–1958, <https://doi.org/10.5194/gmd-9-1937-2016>, 2016.
- Gleckler, P. J., Taylor, K. E., and Doutriaux, C.: Performance metrics for climate models, *Journal of Geophysical Research: Atmospheres*, 113, <https://doi.org/10.1029/2007JD008972>, 2008.
- Hersbach, H., Bell, W., Berrisford, P., Horányi, A., J., M.-S., Nicolas, J., Radu, R., Schepers, D., Simmons, A., Soci, C., and Dee, D.: Global reanalysis: goodbye ERA-Interim, hello ERA5, *ECMWF Newsletter*, 159, 17–24, <https://doi.org/10.21957/vf291hehd7>, 2019.
- Jones, P. W.: First- and Second-Order Conservative Remapping Schemes for Grids in Spherical Coordinates, *Monthly Weather Review*, 127, 2204–2210, [https://doi.org/10.1175/1520-0493\(1999\)127<2204:FASOCR>2.0.CO;2](https://doi.org/10.1175/1520-0493(1999)127<2204:FASOCR>2.0.CO;2), 1999.
- Lange, S.: Trend-preserving bias adjustment and statistical downscaling with ISIMIP3BASD (v1.0), *Geoscientific Model Development*, 12, 3055–3070, <https://doi.org/10.5194/gmd-12-3055-2019>, 2019a.
- Lange, S.: WFDE5 over land merged with ERA5 over the ocean (W5E5), <https://doi.org/10.5880/pik.2019.023>, 2019b.
- Lange, S.: ISIMIP3BASD v2.3, <https://doi.org/10.5281/zenodo.3648654>, 2020.
- Weedon, G. P., Balsamo, G., Bellouin, N., Gomes, S., Best, M. J., and Viterbo, P.: The WFDEI meteorological forcing data set: WATCH Forcing Data methodology applied to ERA-Interim reanalysis data, *Water Resources Research*, 50, 7505–7514, <https://doi.org/10.1002/2014WR015638>, 2014.